OBSERVATIONS OF PERFECT POTENTIAL FLOW AND CRITICAL VELOCITIES IN SUPERFLUID HELIUM II

Thesis by

Paul Palmer Craig

In Partial Fulfillment of the Requirements

For the Degree of

Doctor of Philosophy

California Institute of Technology

Pasadena, California

1959

ACKNOWLEDGMENTS

The author wishes to thank Professor John R. Pellam for suggesting this project and for providing unsparingly of his time from the inception to the conclusion.

The many helpful and interesting discussions with Professor R. Feynman of the Physics Department and Professor P. Lagerstrom, Professor H. Liepmann, and Professor A. Roshko of the Aeronautics Department and their continued interest in the investigation are gratefully acknowledged.

Acknowledgment is made for the joint support by the National Science Foundation and the Alfred P. Sloan Foundation, Inc. of this research.

ABSTRACT

The lift on an airfoil placed in a velocity field of pure superfluid has been found to vanish (i.e., to be at least two orders of magnitude less than the classically expected value) for sufficiently low flow velocities. This result indicates that superfluid helium II can undergo pure potential flow without dissipation. The classical viscosity boundary condition at the trailing edge (Kutta condition) does not apply. Above a (temperature dependent) critical velocity, lift appears. However, even at the highest velocities obtained the observed lift lies far below that expected classically. The critical velocity found from this experiment rises near the lambda point in qualitative agreement with comparable experiments, but fails to show agreement in certain other respects. A "superfluid wind tunnel" capable of developing the required flow is described.

CONTENTS

FIGURES AND TABLE

INTRODUCTION

A variety of experiments have shown that the flow properties of helium II are unique. Most of these experiments may be understood in terms of the two fluid model of helium proposed independently by Tisza (19) and Landau (14), wherein liquid helium cooled below a transition temperature (lambda point) is considered to be composed of two interpenetrating fluids (Appendix I). One of these, the normal fluid, possesses the attributes of a classical viscous fluid while the other, the superfluid, exhibits no viscosity effects whatsoever and should be capable of pure potential flow without dissipation.

Numerous experiments have confirmed the essential correctness of this proposal (2),(6),(9),(10),(11),(21). Helium below the transition temperature (helium II) can be forced through capillaries with an extremely small attendent pressure drop provided the velocities are kept sufficiently low. Disks oscillated in a helium II bath show damping due to normal fluid alone for amplitudes of oscillation below some critical value. At larger amplitudes the flow properties of the superfluid deteriorate and additional damping appears. However, with the exception of some recent experiments with rotating helium (9) no demonstration has been given which shows conclusively that the viscosity of the superfluid component is identically zero. It has only been shown to lie below a particular limit.

It is therefore of considerable interest to devise an experiment capable of indicating qualitatively that the viscosity vanishes identically as distinguished from being immeasurably small.

The mechanism which provides lift on an airfoil allows such an experiment. Circulation of fluid about an airfoil creates a Bernoulli effect reduction in pressure on the upper surface over the lower surface. The effect is independent of the viscosity of the medium and does not require compressibility. However, the presence of the circulation is due directly to viscosity, the interaction occurring through a boundary condition known as the Kutta condition.

In the absence of viscous effects the energy in any region will be minimized for zero circulation. Therefore, lift will not develop about an airfoil. Should there be present any viscosity whatever then dissipative forces acting at the sharp trailing edge of an airfoil where the local velocities are highest will create circulation of such a magnitude as to make the trailing edge velocity vanish. The presence of viscosity alone controls the circulation. Its size does not enter. The flow pattern in the limit as viscosity approaches zero ($\eta \to 0$) is fundamentally different from that appearing for viscosity identically zero ($\eta \equiv 0$).

The present experiment utilizes this fact to show that for sufficiently low superfluid flow velocities the viscosity of superfluid helium II does in fact vanish. As the flow velocity increases dissipative effects eventually appear which cause circulation and hence lift. The observed lift can be qualitatively understood in terms of a critical velocity and a modification of the classical Kutta condition. The temperature dependence of the observed lift and critical velocity thus far have no theoretical explanation.

During the course of experimentation Feynman proposed that the experiment might reveal the existence of quantized vortex elements proposed independently by Onsager (15) and Feynman (8). An investigation was carried out in an unsuccessful attempt to demonstrate the effect. Instrumental difficulties preclude a definite conclusion as to the applicability of this theory to the present experiment.

I.1 SUPERFLUID WIND TUNNEL

a) Description

The experiment was performed in a "superfluid wind tunnel" (16) wherein the normal fluid component of helium II could be immobilized while a uniform flow of superfluid was established. This dynamically synthesized a system at absolute zero, for the normal fluid (excitations) could have no effect upon the wing assembly under investigation.

(Fig. 1) illustrates the tunnel assembly, consisting of the thermally isolated region (R) surrounded by the vacuum jacket (V) and closed at the top by a carborundum seal (S) and at the bottom by a seal (S') of carborundum or other material. Heater (H) above the upper seal provides the motive power for the tunnel by an application of the fountain effect. The superfluid passes upward past the heater where it is partially converted to normal fluid. A mixture in approximate thermal equilibrium with the surrounding bath passes up tube (T) and falls back into the main bath at level (L).

The main test section consists of a cylindrical region 3.0 cm. in diameter and of length 7 to 9 cm. (depending on the sizes of the upper and lower seals). The vacuum region prevents heat currents from disturbing the flow pattern within the test section. An external light shield minimizes radiation effects. Smoothing devices consisting of thin carborundum plugs, fine mesh screens, lengths of parallel tubes, or some combination of these prevented flow instability. The parallel

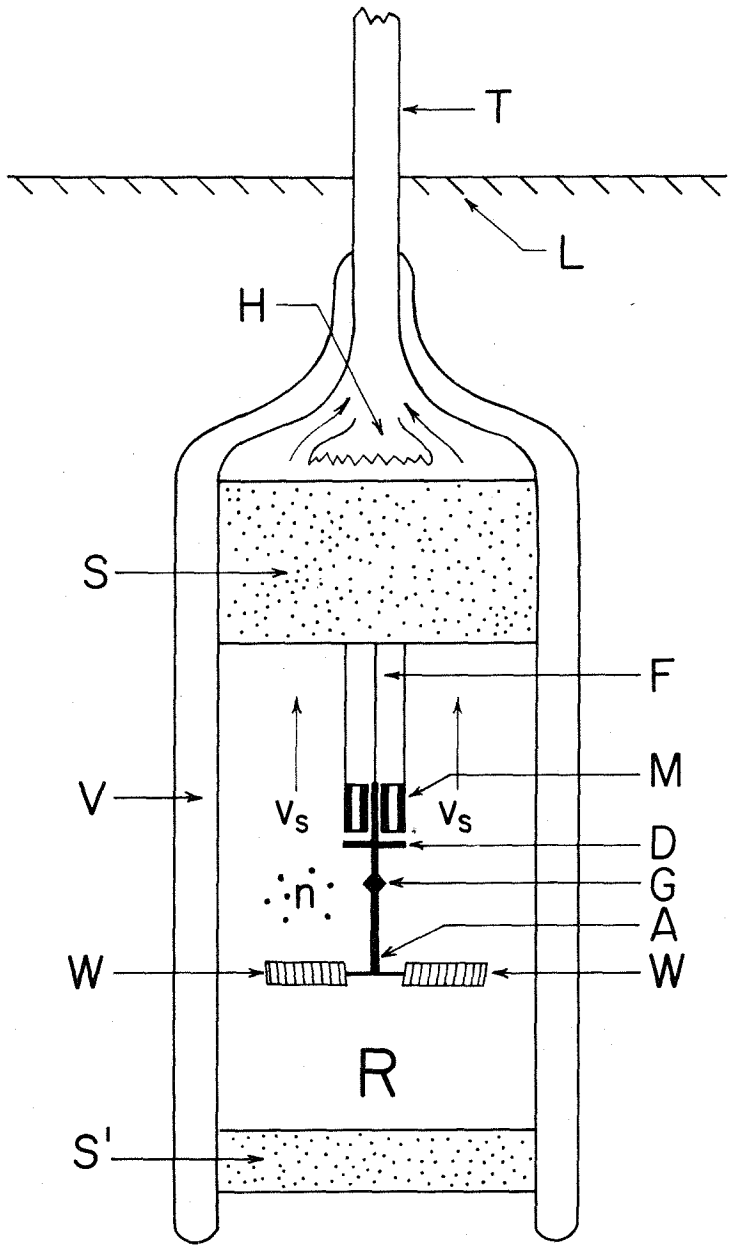

"SUPERFLUID WIND TUNNEL" AND WING ASSEMBLY

Figure 1

tubes seemed best in this respect.*

In certain experiments the test section was constricted to 1.0 cm. by means of tapered lucite inserts. This has the effect of increasing by a factor of nine the maximum flow velocity attainable. For ease in mounting wing assemblies glass sleeves of 2.6 cm. inside diameter were occasionally used.

b) Theory of operation

If there are no heat leaks a quantity of heat (H) (cal) applied to the heater causes the helium level above the heater to rise to a fixed height determined by the fountain effect equation. A continuous heat input ($\dot{H}$) (cal/sec) creates entropy and hence normal fluid. Since normal fluid is incapable of penetrating the carborundum it must move upward. In terms of the fluid entropy (s) (cal/gm-deg), density (ρ) (gm/cc), temperature (T) (^{o}K) and the tunnel area (A_t) (cm^2), the normal fluid particle velocity above the heater (V cm/sec) becomes

$$V = \frac{\dot{H}}{\rho s T A_t} \qquad (1)$$

Within the test region (R) only superfluid can be in motion, while above the upper barrier (S) superfluid is converted to normal fluid at such a rate that the mixture travels with composite velocity (V) (cm/sec). The normal fluid concentration (ρ_n / ρ) corresponds to

* An overall check of the tunnel configuration for uniformity of flow was carried out using water colored with ink. It was found that without smoothing devices at the tunnel throat the flow was highly irregular, whereas with them the flow was smooth and uniform and objects "downstream" from the test section had no influence on the pattern at the test section. Because of the low Reynolds number of this test this cannot be considered a positive indication that the flow of helium II would also be uniform.

a temperature approximately equal to that of the surrounding bath (slightly higher due to the fountain effect), and the two fluids must therefore travel with identical velocities. The superfluid velocity (v_s) (cm/sec) within the test section may be related to the velocity at the heater by momentum conservation:

$$\rho_s v_s = \rho_s V + \rho_n V = \rho V$$

so that

$$v_s = (\rho/\rho_s)V = \frac{\dot{H}}{\rho_s s T A_t} \qquad (2)$$

where $\rho_s \equiv \rho - \rho_n$ (gm/cc) represents the superfluid density. A graph of equation 2 (fig. 2) illustrates the theoretical dependence of superfluid velocity upon temperature.

The temperature of the system is measured in the usual way by means of the vapor pressure. The cryostat temperature must be maintained accurately constant because of the strong temperature dependence of the superfluid velocity.

c) Pitot tubes

If there were no stray heat leaks the velocity could be determined directly from the power input. In practice this method is not sufficient for heat leaks inevitably occur. The thermal conductivity of the glass and the carborundum are finite. Normal fluid leaking backwards through the carborundum carries away heat. Evaporation from the tunnel outlet is a major source of loss. As helium pours out of the tunnel it may establish a path to the main bath down which heat can propagate by second sound. Film transfer introduces a further loss.

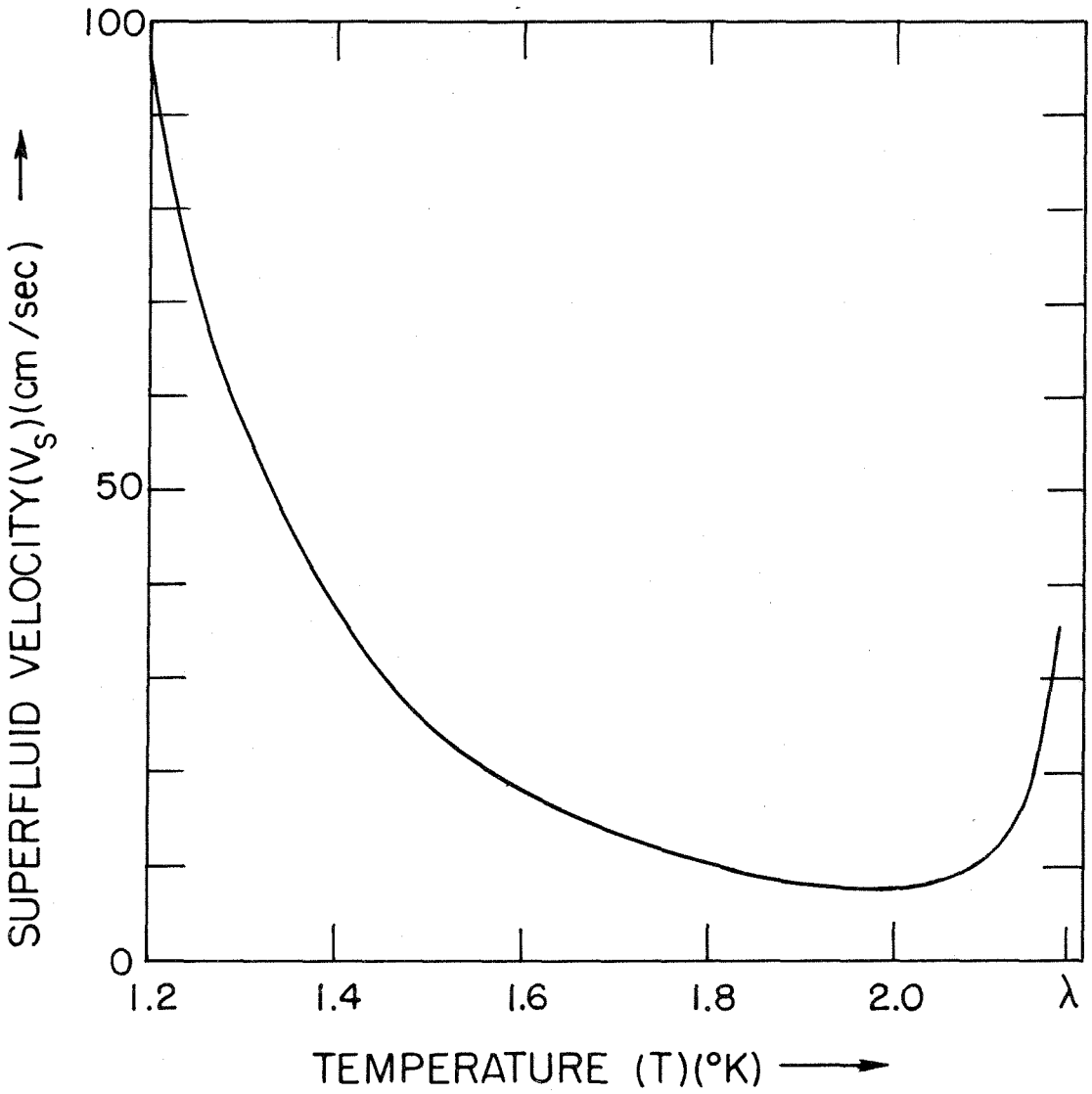

THEORETICAL DEPENDENCE OF SUPERFLUID VELOCITY (V_s) UPON TEMPERATURE (T). (for fixed power input of one watt/cm^2)

FIGURE 2

As the power input to the system is varied to change the velocity the temperature of the helium bath fluctuates, so the velocity must be calculated at each point. Even with an automatic pressure controller fluctuations are appreciable. For large power inputs the flow of superfluid through carborundum saturates so the temperature at the heater rises far above that of the bath. Near the lambda point boiling at the heater may completely obviate a calculation based upon power input.

It therefore becomes desirable to find an accurate independent means for measuring velocity. The pitot tube (fig. 3) meets this need for it provides a measure of velocity independent of density. Static and dynamic pressure measuring tubes are mounted at the same level above the heater (H), so that in reading the difference (h) in the liquid levels frictional effects are avoided.

Assuming both superfluid and normal fluid components to contribute to the pressure reduction in proportion to their densities, the velocity past the pitot tubes (V_p) (cm/sec) may be found from Bernoulli's equation to be

$$V_p = (2gh)^{\frac{1}{2}}$$

where g = 980 cm/sec and (h) is the above level difference in centimeters.

Introducing the cross sectional area at the pitot tubes (A_p) (cm^2) the tunnel velocity becomes

$$v_s = (\rho/\rho_s)\ (A_p/A_t)\ (2gh)^{\frac{1}{2}}$$

For the tunnel used throughout most of these experiments $A_p = 0.0616$ cm^2, $A_t = 7.07$ cm^2 and hence

$$v_s = 0.39\ (\rho/\rho_s)\ h^{\frac{1}{2}} \qquad (3)$$

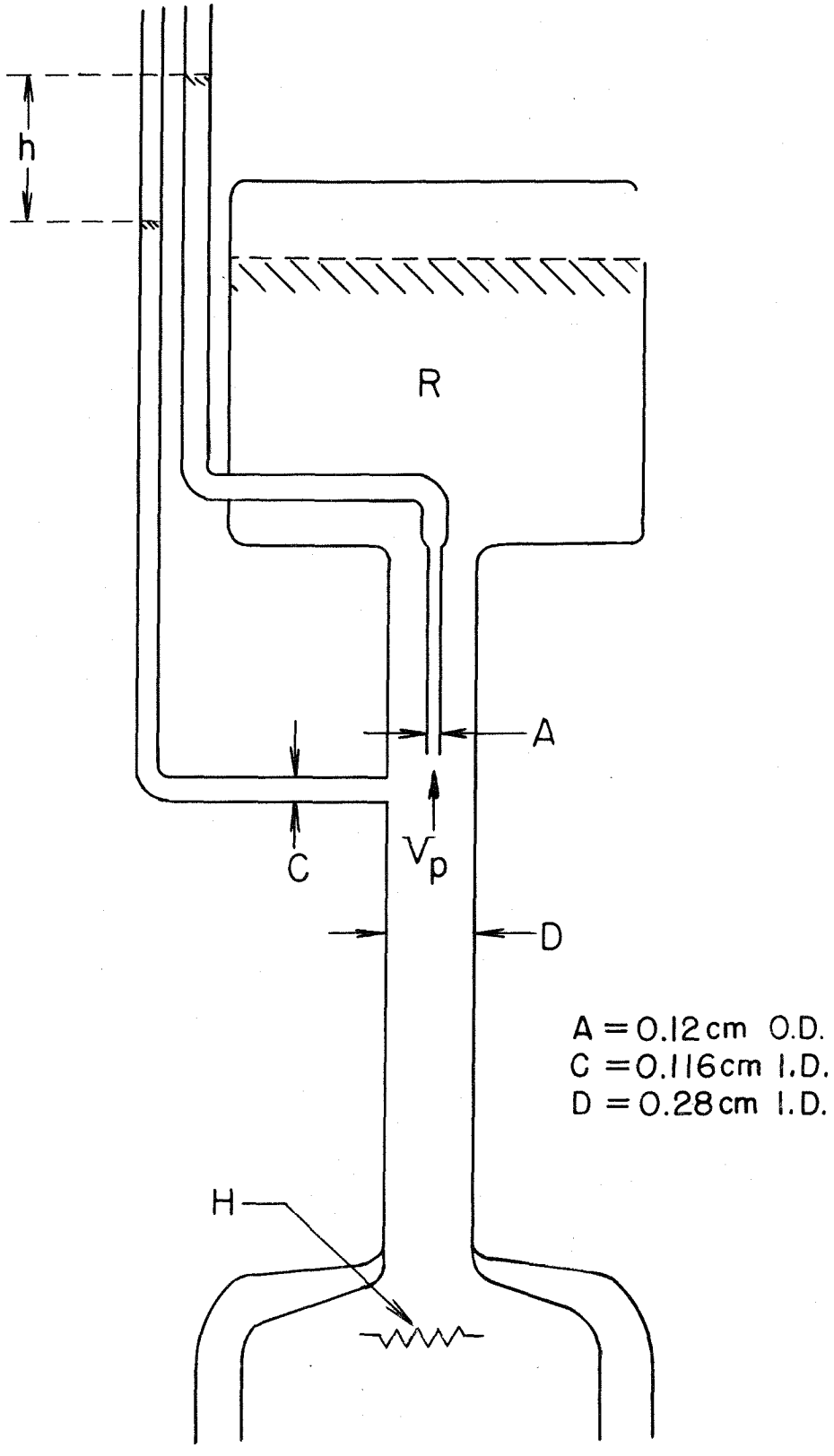

DETAILS OF PITOT TUBE VELOCITY MEASURING DEVICE

FIGURE 3

The validity of this application of Bernoulli's equation to helium II was established experimentally to within about 5% by calibration based on the filling time of a reservoir of known volume (R, fig. 3).

The mechanism by which the pitot tubes operate in helium II has not been fully investigated. Experimentally the system acts as if both superfluid and normal fluid contribute classically and additively to the observed level difference. However, a fluid counterflow probably exists within the pitot assembly due to heat going into evaporation (see e) below). Such flow would be expected to cause a spurious contribution to the observed level difference (h), for the heat would be carried by normal fluid in the same manner as occurs in the "Rayleigh Disk" type of counterflow tunnel (16). Experimental calibration provides adequate justification for the use of pitot tubes as the basic velocity measuring device in the present experiment for it shows that other effects, if they occur, are either not important or are cancelled by other effects. A detailed investigation of the behavior of pitot tubes in helium II might well prove profitable.

d) Fluctuations

At high tunnel velocities rapid fluctuations are observed in the levels read in the pitot tubes. Their amplitude increases with flow velocity to a maximum of several millimeters at the highest velocities obtained and for the lowest temperature of about 1.3°K. No quantitative study was made of the temperature dependence of the fluctuations, although it was observed that at higher temperatures their amplitude decreased. The fluctuations are probably coupled to the main test section of the tunnel where they may be observed as instability of the system

under test, although possibly other causes contribute more strongly to these instabilities. Should the amplitudes of oscillation at the pitot tubes correspond directly to changes in the tunnel flow they would imply variations of up to several millimeters per second in the superfluid flow velocity.

It was suspected that the effect might be caused by boiling on the resistor or by helium dripping erratically from the tunnel into the main bath thereby causing intermittant thermal contact between the bath and the heater. Modifications of the resistor shape and of the tunnel had negligible effect upon the noise. No method has been found to appreciably change these fluctuations, which probably constitute one of the major difficulties in the operation of the tunnel, since random fluctuations in the orientations of the wing assemblies limit the ease and accuracy of measurement. These noise effects are felt to be the prime cause of the inconclusive results of the investigation into the quantization of lift (see Part III.3).

e) Heat leakage

Using the pitot tube as a standard the accuracy of velocity computed from power input could be ascertained. In (fig. 4) we plot the superfluid velocity computed from power input versus that found from the pitot tubes.* The dashed curve has been drawn with unity slope, but with the ordinate chosen for optimal fit to the data. The axis intersection at 0.23 cm/sec corresponds to an "excess" heat input producing no measurable mass flow at the pitot tubes (i.e. the power

* The velocity given is that possessed by the superfluid immediately before entering the carborundum barrier.

input necessary merely to hold the helium at a fixed height in the reservoir, with no overflow). Data are plotted for several representative temperatures (indicated by different symbols) corresponding to a wide range of superfluid densities. Although the heat input producing a superfluid velocity of 0.23 cm/sec varies widely with temperature (fig. 2), all observations lie on the dashed line. This result holds to within an experimental error of about ± 10% over the entire temperature range investigated (1.3°K to 2.1°K).

The reason for the correspondence of the "excess" heat to a fixed superfluid velocity remains unexplained. At a fixed temperature evaporation from the reservoir (R, fig. 3) could suffice. The approximately fixed height of the reservoir above the helium bath implies that a temperature difference (due to fountain effect) exists between the bath and the reservoir. This implies an excess vapor pressure above the reservoir and an attendent evaporative heat loss.* However, the temperature dependence predicted by such a model fails to agree with that observed, so that some additional and at present unknown mechanism must be operating.

Heat leakage through the carborundum would change the observed slope of (fig. 4), modifying the equations of motion of the tunnel and consequently the lift curves obtained with the airfoil. To make a first order approximation to the effect of such leakage we assume a certain temperature dependent amount of heat (H_o (T)) corresponding to a fixed

* The vapor pressure difference between the bath and the reservoir may be found from the vapor pressure curve for helium once the temperature difference has been determined from the fountain effect equation. The evaporative power loss may be expected to be proportional to this vapor pressure difference.

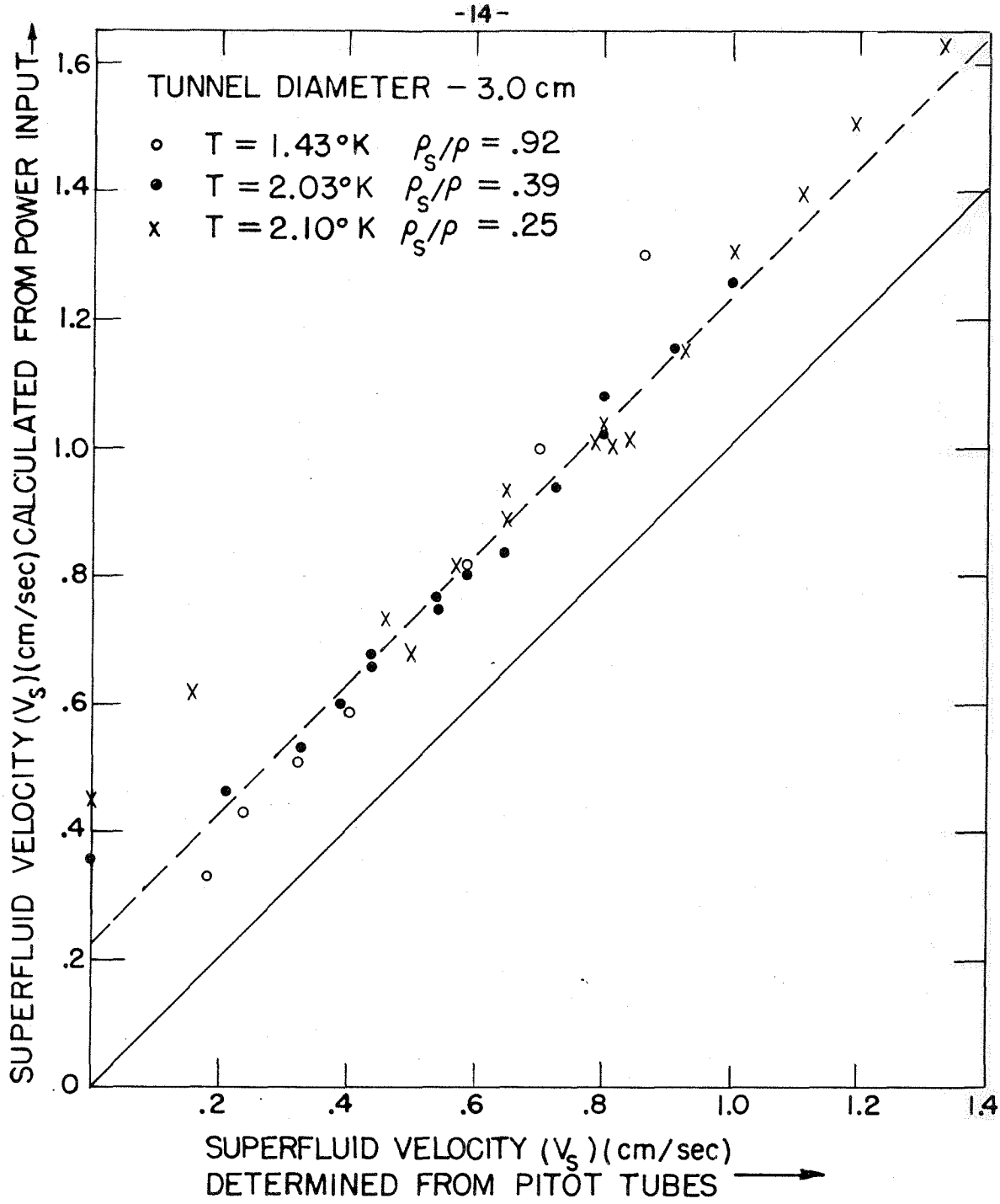

SUPERFLUID VELOCITY, THEORETICAL VERSUS MEASURED (PITOT TUBE)

THE SOLID LINE ASSUMES NO LOSSES. THE DASHED LINE REPRESENTS THE BEST FIT WITH SLOPE UNITY, AND APPLIES AT ALL TEMPERATURES

FIGURE 4

superfluid velocity (v_1) is lost due to heat leakage through the glass, evaporation, film flow, etc. Of the remaining heat a major fraction (γ_o) will be used in the usual superfluid tunnel manner, and the remaining (small) fraction ($1-\gamma_o$) will supposedly leak through the carborundum, to produce normal fluid counterflow within (R) (fig. 1). In terms of (γ_o), the normal fluid concentration ($\rho_n/\rho = x$), and the superfluid velocity (v_{sp}) calculated from the pitot tubes, the actual flow velocity of superfluid becomes (Appendix V):

$$v_s = \left[1-\left(\frac{1-\gamma_o}{\gamma_o}\right)x\right] v_{sp} \qquad (4)$$

and the normal fluid counter flow velocity is

$$v_n = \left[\left(\frac{1-\gamma_o}{\gamma_o}\right)(1-x)\right] v_{sp} \qquad (5)$$

The reciprocal of (γ_o) equals the slope of (fig. 4).

These are the superfluid velocity and the reverse normal fluid velocity which are expected to exert forces upon apparatus placed within the tunnel. From graphs similar to (fig. 4) one finds that the velocity determined from the pitot tubes does not deviate by more than about 10% (appearing as deviations from unity slope) from that determined from heat input after the additive leakage constant has been subtracted. On this model the ratio of normal fluid velocity to superfluid velocity reaches a maximum of 0.11 at $x = 0$ for a heat leakage of 10%. Thus the superfluid velocity must at all temperatures exceed that of the normal fluid by a factor of at least 9. Since with the test section of diameter 3.0 cm. the maximum superfluid flow velocity obtainable is 1.8 cm/sec, the maximum normal fluid velocity cannot exceed 0.2 cm/sec, and will be less in the low velocity range often of interest.

It should be emphasized that not all of the fractional leakage is necessarily lost through the carborundum. This assumption represents the worst case, and thus allows establishment of an upper bound on any experimental effect which might be due to leakage of this type. The only way in which the effect of leakage within the test section might be greater than that predicted above would be if some competing effect should reduce the apparent leakage. Although no mechanism capable of accomplishing this has been suggested, the "negative lift" results described in Part II.1b suggest that other effects are present.

f) Flow within the test section

The detailed structure of the flow within the test section is difficult to estimate. The filters at the entrance of the tunnel contribute to smoothing of the superfluid flow, as do various constrictions which may be placed within the test section. However, the details of the superfluid flow pattern cannot be investigated, and may be quite uneven within the test section. The same holds true of the normal fluid counterflow, which can be taken into account only if smooth and uniform. Should the heat source for the counterflow prove irregular, countercurrents would result leading to random oscillations of any assembly placed within the tunnel.

By changing the position of airfoils within the test section it may be demonstrated that should any appreciable steady state irregularity exist it must be confined to the vicinity of the tunnel walls (Part II.1d). The observations in the central part of the tunnel were independent of the location of the wing assemblies with regard to the tunnel. A counterflow sufficiently homogeneous to effect the airfoil

equally regardless of orientation would not have been detected and would influence the results. Since the total fractional heat leakage within the system was only about 10% (see e) above) such effects are probably not appreciable, but may be responsible for the reverse deflections noted (Part II.1b).

Calculation of the superfluid velocity is based upon knowledge of the temperature within the test section. Should an efficient thermal barrier be inadvertantly introduced at the lower end of the test section (S', fig. 1), the temperature within the test section would bear no simple relation to that of the surrounding bath, and could even rise above the lambda point. Good thermal conduction from the test section to the surrounding bath must be provided.

g) Usefulness of the superfluid wind tunnel

The superfluid wind tunnel described in principle produces a flow of pure superfluid with the normal fluid completely immobilized. This ideal behavior may be approached in practice, subject to certain limitations. Fluctuations in the flow velocity (d above) preclude strictly steady state measurements. Reverse heat leakage through the tunnel (e above) creates a counterflow of normal fluid which may cause difficulty in sensitive measurements. Non-uniform flow within the test section (f above) may cause high local velocities and turbulence effects which are virtually impossible to study or eliminate, but which may influence experiments.

If these factors are taken into account the superfluid wind tunnel may prove a powerful tool for the investigation of the flow properties of helium II.

I.2 WING CONSTRUCTION

a) Configuration

The lift forces expected from wings of a size chosen to fit inside the wind tunnel and operating at available velocities are extremely small, making it necessary to design the apparatus to attain an ultimate in sensitivity. This was done by utilizing torque rather than force measurement. The lift due to a pair of wings mounted at equal and opposite angles of attack created a couple which could be converted to an angular deflection with a torsion fiber. By measuring the deflection of the assembly with an optical system the lift forces could be found. The sensitivity using the finest fibers was a torque of 5 microdyne-cm corresponding to forces of the order of 5 microdynes.

The mechanical arrangement is shown in (fig. 1), where a pair of wings (W) are attached at opposite angles of attack to the ends of a crossarm (A) suspended from a fiber (F). An eddy current damping device consisting of a copper disk (D) mounted on the wing assembly and fixed permanent magnets (M) served to damp out oscillations. The one millimeter square mirror (G) allowed optical angular measurements of system deflections to an accuracy of one half degree.

b) Materials and assembly

Wings were constructed of a variety of materials in a variety of shapes. From an experimental viewpoint the most successful configurations consisted of thin flat strips, for assemblies fabricated of these possessed low moments of inertia and therefore permitted rapid measurements. Other wings had large chord-to-thickness ratios in an attempt to approximate elliptical cross sections. Materials used were

quartz, mica, wood, pyrex, and fly wings. The fly wings came closest to approximating the form of commercially successful wings but since the geometry was not known it was difficult to make comparisons with theory. The constructional details of a typical mica wing assembly are shown in (fig. 5).

The wing components were immobilized in a brass jig during glueing and fusing operations. Mica wings were assembled with diluted Duco cement while the pyrex and quartz wings were fused. Duco provided the means for attachment of the fibers.

c) Suspensions

Suspensions consisted usually of quartz fibers and occasionally of phosphor bronze strips. The torsion constant for a particular wing assembly was chosen experimentally to give the desired angular deflection with the flow velocities available. Values used ranged from about 10^{-1} to 10^{-4} dyne cm/rad.

Fibers were drawn from 3 mm diameter stock, and stored in a closed container attached to paper tabs giving the approximate torsion constants. Accurate calibration before installation involved timing the fibers as torsion pendula using a standard moment of inertia. At liquid helium temperatures the torsion constants of quartz fibers were found unchanged from their values at room temperature.

d) Damping

In order to eliminate noise effects which were manifest as random oscillations of the wing assembly, a magnetic damping device was incorporated consisting of six Cunife magnets (M in fig. 1). These were arranged to form six dipoles mounted rigidly inside a pyrex

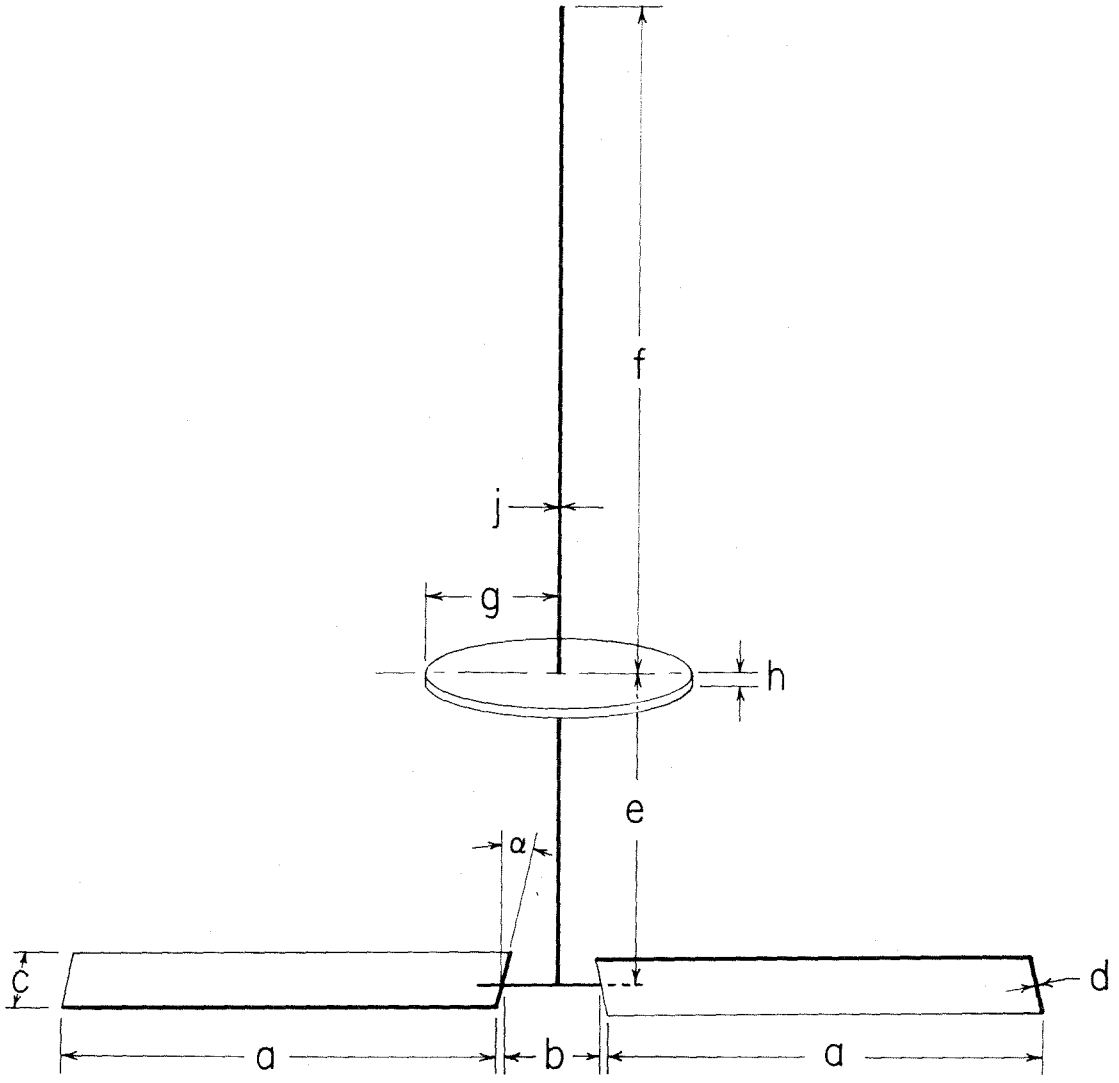

a - 1.00 cm
b - 0.20 cm
c - 0.14 cm
d - 0.0056 cm
e - 0.70 cm
f - 1.50 cm
g - 0.30 cm
h - 0.02 cm
j - 0.036 cm
α - 20 degrees

MICA WING ASSEMBLY

Figure 5

sleeve and "downstream" from the wings so the superfluid passed over the wings before reaching them, thus avoiding distortion of the flow pattern. Spacing of about one half millimeter between the disk and magnets gave maximum damping yet avoided any possibility of rubbing due to misalignment. The copper used in the damping disks was selected for purity so that the resistivity dropped to a low value at helium temperatures, assuring adequate damping.

e) Techniques

Assembling the wings was at best tedious, but was facilitated by a well equipped micromanipulator room. A Zeiss binocular microscope with magnification variable from 10X to 80X and a calibrated reticle was a major piece of equipment. A special mount giving complete freedom of motion in the horizontal plane allowed involved assembly processes to be followed.

The micromanipulators consisted of Brinkman bases with micrometer adjustment in three perpendicular directions, upon which were mounted Neher type arms (18) providing universal motion in preliminary alignment and serving to hold various probes.

A gas-oxygen or oxy-hydrogen microtorch constructed from a hypodermic syringe mounted on a blast furnace universal base allowed fusing of small pieces of quartz or pyrex. Hypodermic needles provided tips in all sizes needed.

I.3 AIR CALIBRATION TUNNEL AND NORMAL FLUID TUNNEL

a) Air calibration

Due to wall interactions theoretical calculations of the classical lift expected from airfoils placed within a cylindrical tunnel such as the superfluid wind tunnel are virtually impossible. Consequently air calibration was employed. This calibration was accomplished by placing the entire wing assembly within a glass sleeve of inside diameter equal to that of the superfluid test tunnel and forcing air past the assembly. The air volume flow was measured using a rotameter and converted to flow velocity.*

The torque was observed to depend quadratically upon the velocity, as predicted by the classical theory. In Part III.1 it will be shown that classically the lift force and hence the torque on a given airfoil is related to the particular fluid under study through a quadratic velocity dependence and a linear density dependence. Thus the results obtained in the air tunnel could be converted directly to those expected from a classical fluid of density equal to that of superfluid simply by multiplication by the density ratio, the higher density fluid exerting the greater torque at a given velocity.

The accuracy of these measurements was low, so that deviations of ± 10% were easily possible in the deflection and velocity measurements. Errors introduced by uncertainties in the centering of the wing

---

* Assuming the air flow velocity to be constant over the tunnel section. An accurate calculation would include the velocity distribution across the section. Comparison between the lift obtained assuming a constant velocity distribution and the theoretical value assuming infinite aspect ratio may be made using columns 10 and 11 of Table 1 (Part II.1c).

in the tunnel could well have been larger and are not easily detectable.

b) Normal fluid

An independent investigation, not related to the main project, concerned the lift exerted on a wing placed in a flow of the normal fluid component of helium II. While there was little doubt as to the outcome of such an experiment, it was none the less of interest to demonstrate experimentally that the behavior of normal fluid follows that expected classically.

The experiment was performed with wing #6 (see Table 1) mounted in a vertically oriented counterflow wind tunnel of the type used in the first investigation of the Rayleigh disk (16). No damping was used on the wing assembly. The torsion constant of the suspension was 1.39 millidyne-cm/rad. Since the net momentum within a counterflow system vanishes, it follows that at sufficiently low temperatures the kinetic energy associated with the normal fluid greatly exceeds that associated with the superfluid (by a factor of 19 at the operating temperature of 1.3°K where $\rho_s/\rho = 0.95$), thereby permitting the investigation of the effect of normal fluid alone independent of the superfluid properties. Since at low superfluid flow velocities we shall show that the lift exerted by superfluid falls far below that expected classically, we are assured that the results observed are substantially due to the normal fluid.

In (fig. 6) are presented the results of the experiment. The normal fluid velocity (v_n) is obtained from power input to the tunnel. The solid curve represents the result of air calibration converted to the density of normal fluid at 1.3°K ($\rho_s = 0.138$ gm/cc). The

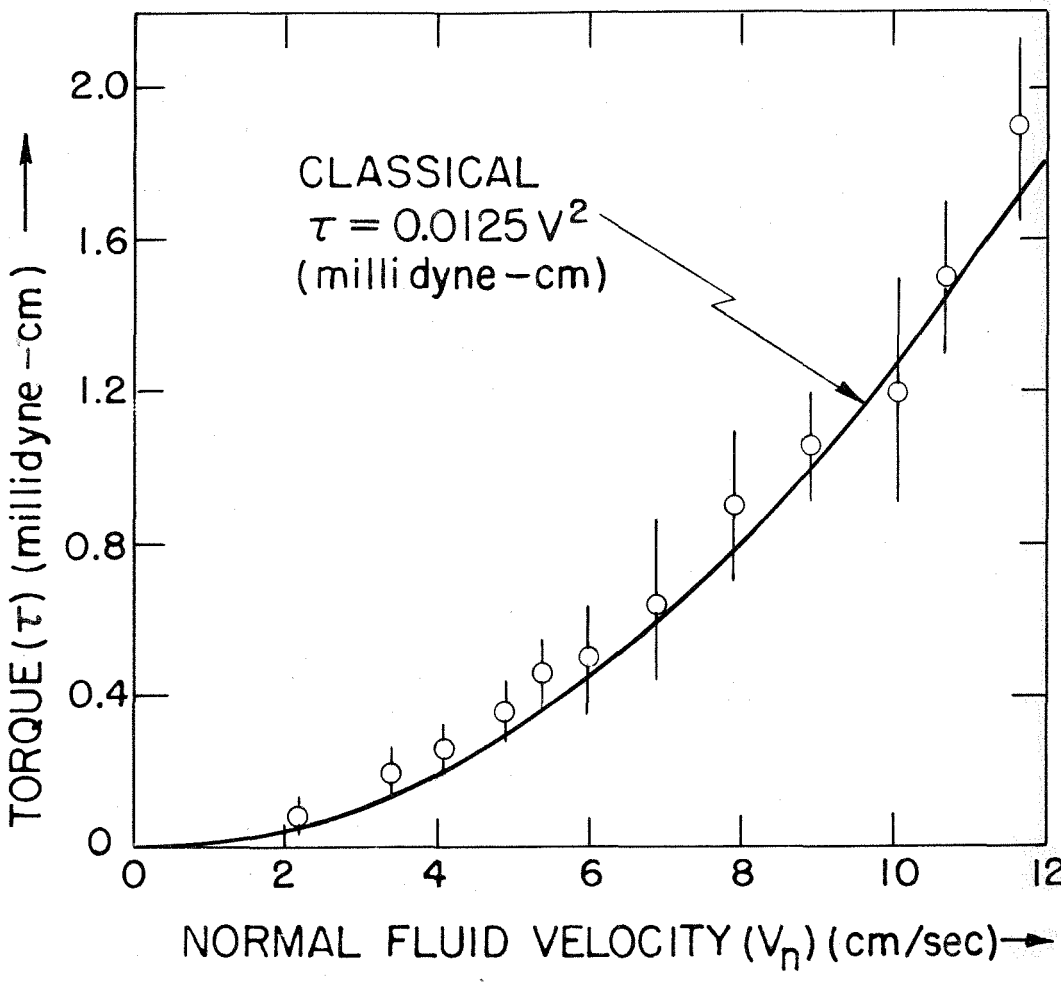

TORQUE (τ) ON WING ASSEMBLY VERSUS NORMAL FLUID VELOCITY (V_n) ($T = 1.3°\,K$)

FIGURE 6

experimental points indicate the torques exerted on the wing assembly for various normal fluid flow velocities (v_n) obtained from the power input to the tunnel. The effect of superfluid (flowing in the opposite direction to the normal fluid) has been neglected. Within an experimental accuracy of about 10% the observations agree well with the classical expectations. While this result was checked only at a temperature of 1.3°K no reason has been suggested for expecting deviations to occur at other temperatures.

The wide spread in the experimental points in (fig. 6) is due to oscillations in the undamped wing assembly. Since there was no superfluid seal used in this wind tunnel the instability must be due to some other factor. The amplitudes of the oscillations are roughly the same fraction of the total deflections as observed in the superfluid wind tunnel. This provides an indication that the instability may be due to classical phenomena not related to superfluid flow directly. We shall refer to this point in Part III.3 in analyzing the non-appearance of quantized lift in the superfluid tunnel.

II EXPERIMENTAL RESULTS

Introduction

Experimental runs consist of determinations of the torque exerted on wing assemblies of the type illustrated in (fig. 5) as a function of the superfluid flow velocity within the wind tunnel. Angular measurements are accomplished with an optical system capable of resolution to within $\frac{1}{2}$ degree. Velocities are determined to an estimated accuracy of 5% (excluding leakage effects) using the pitot tube attachment of the superfluid wind tunnel. The results are most easily represented by graphs of the torque (τ) on a wing assembly plotted against the superfluid velocity (v). (Note that the subscript "s" denoting "superfluid" has been deleted; henceforth (v) will be used to represent superfluid velocity.)

These graphs have been obtained for several wings at fixed temperatures, and for a few wings as a function of temperature. In Part II.1 we present the fixed temperature results and in Part II.2 the temperature dependent results.

II.1 EXPERIMENTAL RESULTS - FIXED TEMPERATURE

a) High Velocity Region

For flow velocities greater than some critical velocity (v_c) the observations could in all cases be represented by the semiempirically obtained expression (to be derived in Part III.2)

$$\tau = av(v-v_c) \qquad v \geq v_c \qquad (6)$$

Here the constants (a) and (v_c) are to be determined experimentally. In order to illustrate the form of the results, we present in (fig. 7) the high velocity observations for the wing of (fig. 5) at a temperature of 1.3°K. This is wing #1 on the chart to be presented later (Table 1). The solid line represents the best fit to equation 6. The dashed curve represents the classically expected lift, as obtained from calibration in an air tunnel, converted to the density of superfluid helium at 1.3°K ($\rho_s = 0.95\rho = 0.138$ gm/cc). For velocities below 6 mm/sec no deflection could be noted.

Fitting of equation 6 to the data is accomplished by drawing visually the best straight line through a graph of (τ/v) versus (v). The uncertainty in the slope of such lines has been found to be less than $\pm$ 10% for a given run, although poor reproducibility of the data from run to run requires assignment of an error of possibly $\pm$ 20%. Values of (v_c) obtained are in most cases valid to within better than $\pm$ 1 mm/sec.

Data were obtained for both increasing and decreasing velocities in order to investigate the presence of hysteresis effects. No evidence for such an effect was observed.

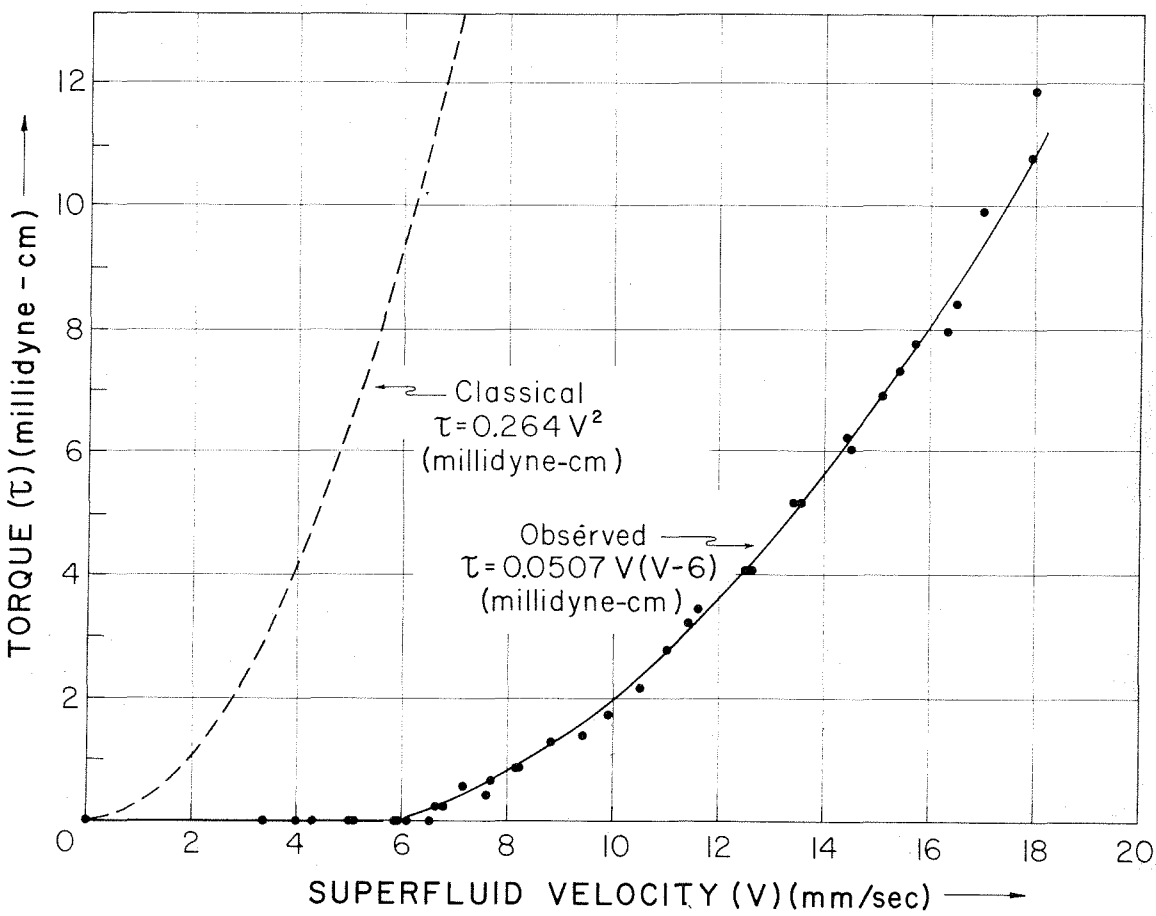

TORQUE (τ) ON WING ASSEMBLY VERSUS SUPERFLUID VELOCITY (V)

Points represent experimental values of torque (τ) found from wing assembly deflection plotted against superfluid velocity (V) found from pitot tubes. The solid curve represents an empirical fit to the data. The dashed curve shows the corresponding classical behavior of the wing assembly.

Figure 7

b) Low velocity region

The details of the low velocity region were studied using much finer suspensions. In (fig. 8) are presented the results for the wing discussed above (wing #1 of Table 1). The suspension used possessed a sensitivity 25 times greater than that used to obtain the data of (fig. 7). With the resolution increased to this extent a negative torque was observed for velocities between about 2.5 and 6 mm/sec.

As the velocity increases above 6 mm/sec the torque exerted on the wing assembly increases extremely rapidly. The point of axis crossing is defined in this particular case to well within $\pm$ 0.5 mm/sec superfluid velocity.

Negative deflections were observed with all wings provided sufficiently fine fiber suspensions were employed.

c) Summary of data

A variety of data has been obtained for various wings. Table 1 presents this in tabular form. Data presented include the dimensions of the wing and tunnel assemblies, the calibration data, and the results in the superfluid tunnel. Both theoretical and experimental calibration data are provided, and have been expressed in terms of the superfluid density at the operating temperature. The coefficients in equation 6 are given, the point where the deflection starts negative, and the maximum negative torque observed. Where no data are indicated none were obtained.

d) Discussion

The accuracy of the experimental data may be questioned primarily with regard to duplicability. Wings with small wall clearance tended to

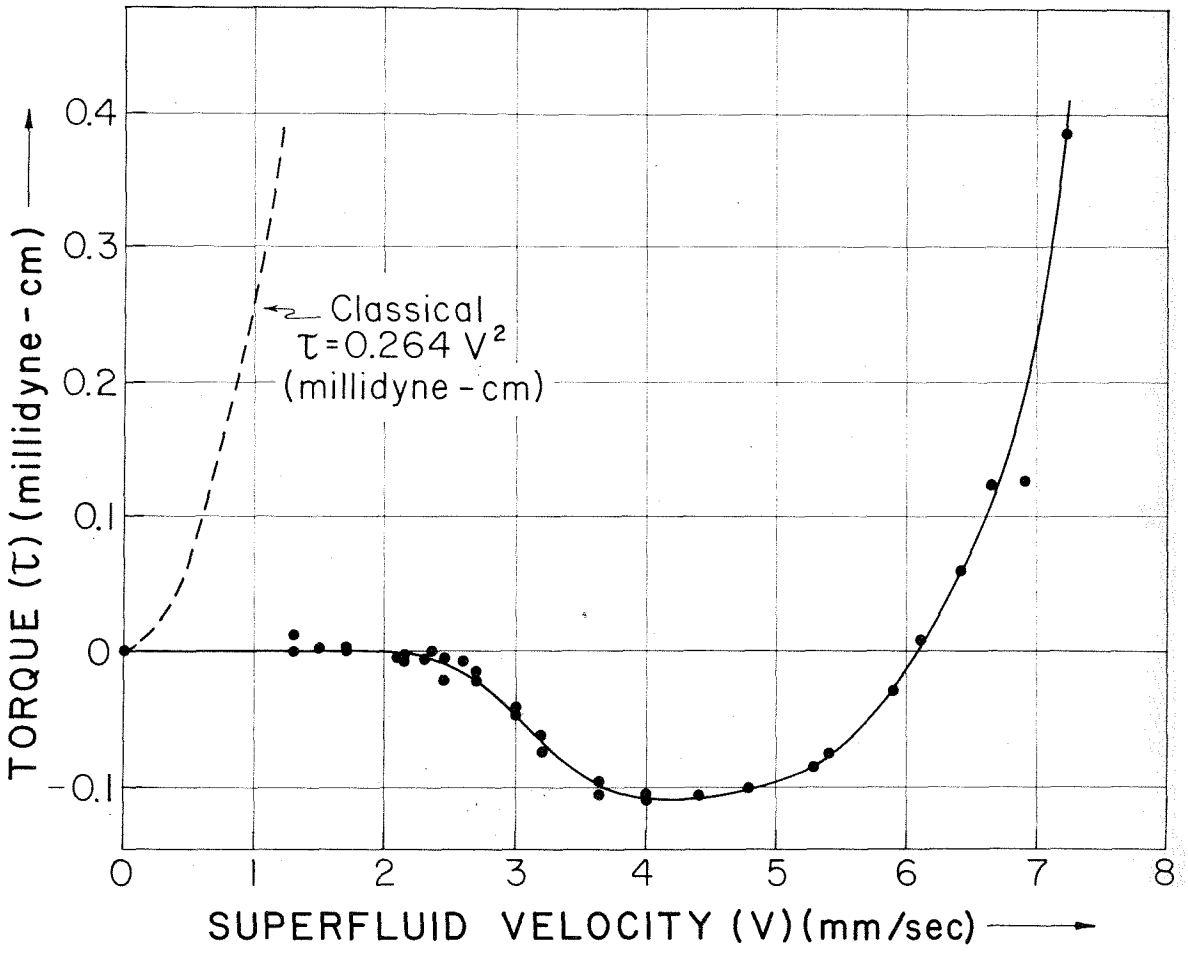

TORQUE (τ) ON WING ASSEMBLY VERSUS SUPERFLUID VELOCITY (V). "HIGH RESOLUTION" DATA

Figure 8

SUMMARY OF FIXED TEMPERATURE DATA
(see notes on next page)

Column	1	2	3	4	5	6
Wing Number	Material	Chord (mm)	Thickness (mm)	Span (mm)	Spacing Between Wings(mm)	Attack Angle (degrees)
1	mica	1.4	0.056	10	2	20
2	mica	1.4	0.056	10	2	4
3	mica	4.2	0.04	12.4	0	4
4	mica	8.0	0.075	11	2	19.5
5	mica	1.75	0.051	9.8	0	4
6	quartz	0.45	0.05	4.2	0	4
7	quartz	0.45	0.05	13	0	4
8	wood	2.92	0.99	10.3	0	4

Column	7	8	9	10 (a)	11 (b)
Wing Number	Tunnel Diameter (mm)	T°K	ρ_s/ρ	Classical Torque Coefficient (α) (Theoretical)	Classical Torque Coefficient (α') Experimental)
1	26	1.3	0.95	260	264
2	26	1.3	0.95	47.5	100 (c)
3	30	1.3	0.95	195	148
4	30	1.3	0.95	1550	960
5	26	1.6	0.825	45	42
6	10	1.4	0.925	2.3	2.3
7	30	1.4	0.925	22	35 (c)
8	26	1.3	0.95	93	43

Column	12 (d)	13 (e)	14 (f)	
Wing Number	Deflection	Maximum Negative Torque (microdyne-cm)	Torque in Helium Tunnel (v_c)(mm/sec)	(a)
1	2.5	120	6	50.7
2	3.0	70	6.5	22
3	2.0	880	8	-
4	-	-	2.75	530
5	4.0	585	14	-
6	10.0	200	52	0.31
7	3.0	220	12.5	-
8	4.0	150	8	7.2

Notes to Table 1

a) The theoretical classical torque coefficient (α) is defined by the equation $\tau = \alpha v^2$ microdyne-cm (v in mm/sec). The density used is that of the superfluid at the operating temperature.

b) The experimental classical torque coefficient (α') is defined by the equation $\tau = \alpha' v^2$ microdyne-cm (v in mm/sec). The density used is that of the superfluid at the operating temperature. The coefficients were obtained from air calibration using the technique described in Part I.3a.

c) The experimental coefficient appreciably exceeds the theoretical coefficient. The reason for this is unknown.

d) The superfluid flow velocity at which observable negative deflections first appear.

e) The maximum negative torque observed (microdyne-cm). The velocity corresponding to this torque is approximately the average of the velocity given in column 12 and that given in the first column of column 14.

f) The observed torque in superfluid may be represented above a critical velocity (v_c) by $\tau = a\, v(v-v_c)$ microdyne-cm (v in mm/sec) (see equation 6).

yield results which varied widely as the orientation of the wing system within the dewar was altered. This effect is due either to large wall interactions or to non-uniform flow within the test section in the neighborhood of the walls. Provided the spacing between wing tips and wall was large in comparison to the wing chord, little difficulty was experienced along these lines. Under these circumstances the data were reproducible to within 10% over several runs, with the equipment disassembled between runs.

However, the important factors are probably not the absolute magnitude of the numbers, but rather the approximate size of the factor by which the observed lift lies below that expected classically. For velocities below the critical velocity (v_c) the observed lift is zero or negative, and hence lies arbitrarily far below the classical lift. Even for velocities far above (v_c) the observed lift lies quite far below the classical. Thus from (fig. 7), at a velocity of 12 mm/sec the observed lift is less by a factor of 10 than the lift exerted on the same airfoil by a classical fluid of the same density.

The mechanism of reverse leakage described in Part I.1 can influence the results only slightly and is inadequate to explain the reverse leakage effects. In Part I.1 it was shown that the leakage flow velocity reaches a maximum value of about 10% of the superfluid velocity. We can estimate the maximum contribution to the negative lift using the classical equations to be developed in Part III.1. Using the normal fluid density of 5% the negative torque on wing #1 (figs. 5 and 8) becomes at a superfluid flow velocity of 10 mm/sec

$\tau = \alpha'(\rho_n/\rho_s)(0.1v)^2 = (0.264)(0.05)(1.0)^2 = 0.013$ millidyne-cm while the maximum negative torque obtained slightly exceeds 0.1 millidyne-cm. In order to explain the observed negative torque using this model for tunnel leakage, we would require a reverse normal fluid leakage velocity of about 50% of the superfluid velocity. This much leakage cannot possibly be justified on the basis of the model presented in Part I.1. In addition the negative deflections do not appear before some finite velocity is reached, and do not possess the parabolic form predicted by the model. This leads to the supposition that some sort of nonlinear leakage effect may be playing a role. Thus far no mechanism has been found to explain the phenomenon.

At present no adequate explanation can be given for the negative deflections. However, the observation that when positive deflections do occur they occur rapidly and exceed the maximum negative deflection within a velocity change of only about 1 mm/sec suggests that the negative deflections are spurious and probably due to a reverse flow of normal fluid. This flow must vary in some nonlinear way with the superfluid flow velocity. Even should we suppose that the negative deflections obscure some positive deflection at low velocities, the classically expected positive torques exceed by about two orders of magnitude the maximum negative torques observed.

Further, at the lowest velocities (below the velocity where negative deflections first occur) zero torque is observed at finite superfluid velocity. This observation, too, leads to the condition that the classically expected torque exceeds the observed torque by about two orders of magnitude.

We feel therefore that the conclusion may be inferred that lift exerted on airfoils by a flow of pure superfluid lies for some velocity range at least two orders of magnitude below the lift expected classically.

II.2 EXPERIMENTAL RESULTS - TEMPERATURE EFFECTS

Data were obtained in the superfluid wind tunnel for several wing assemblies as a function of temperature. In obtaining such data care was necessary to avoid effects due to placement of the wing assemblies in the tunnel. These effects were minimized by cross checking points for reproducibility.

(Fig. 9) presents the critical velocity (v_c) (see equation 6) for wing #5. The critical velocity rises sharply near the lambda point and rises shallowly at low temperature with a broad minimum at about 1.95°K where the superfluid and normal fluid concentrations are equal. (Fig. 10) presents similar data for wing #6. The rise at the low and high ends of the temperature scale are apparent but not as pronounced. Data with other wings showed the characteristic rise in critical velocity at the lambda point. The rise at the low temperature end was not always pronounced.

Difficulty in obtaining this data prevents a final conclusion as to the detailed form of the critical velocity (v_c). Although the curves appear not to be independent of wing geometry, the minimum remains at about 1.95°K. Since the temperature dependence of the critical velocity offers the most obvious means of comparing this experiment with other experiments (Part IV) additional investigations along these lines might prove profitable.

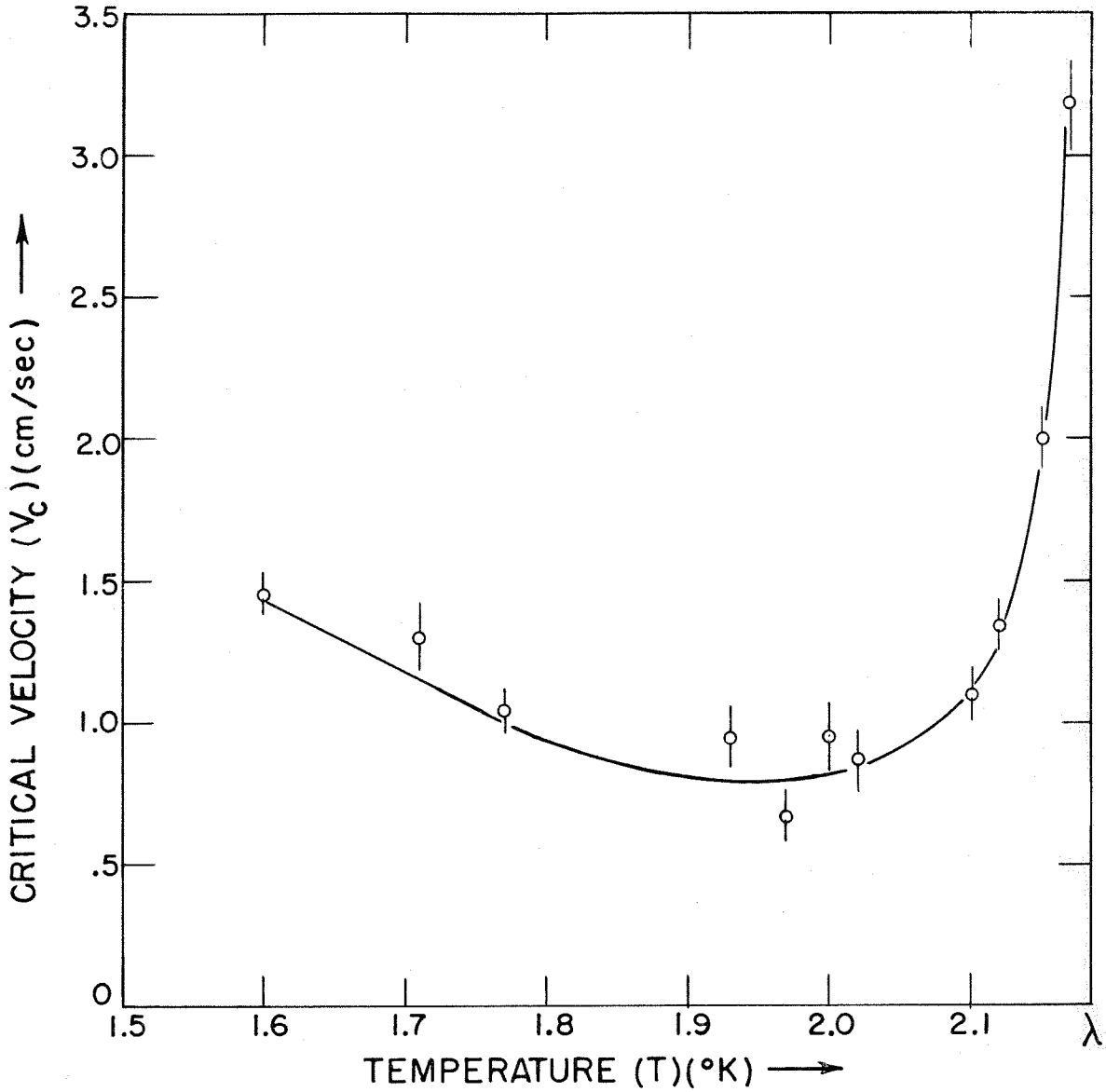

SPAN 0.98 cm / wing
CHORD 0.175 cm
THICKNESS 0.0051 cm

ATTACK ANGLE 4°
TUNNEL DIAMETER 2.6cm
MATERIAL MICA

FREE STREAM CRITICAL VELOCITY (V_c) OF SUPER-FLUID VERSUS TEMPERATURE (T)

FIGURE 9

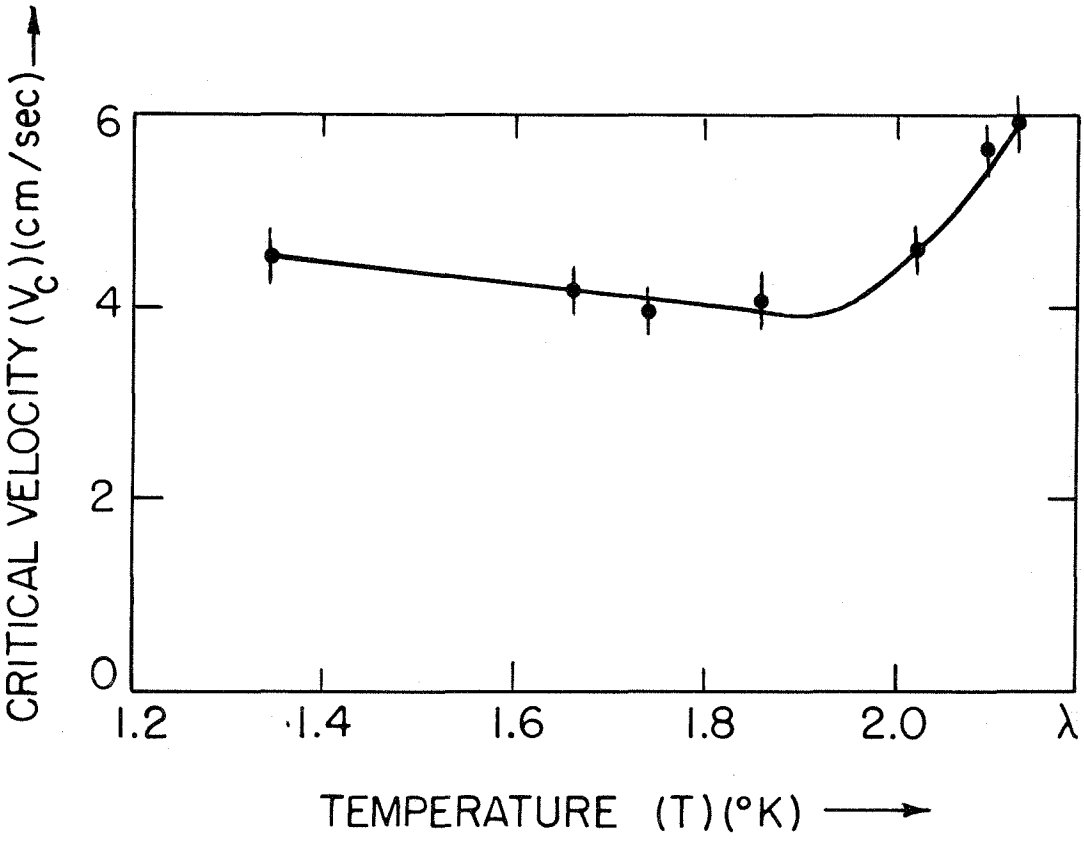

SPAN 0.42 cm/wing
CHORD 0.045 cm
THICKNESS 0.005 cm

ATTACK ANGLE 4°
TUNNEL DIAMETER 1.0 cm
MATERIAL QUARTZ

FREE STREAM CRITICAL VELOCITY (V_c) OF SUPER-FLUID VERSUS TEMPERATURE (T)

FIGURE 10

III THEORY - INTRODUCTION

The basic motivation for this experiment was an investigation into the vanishing of viscosity within the superfluid component of helium II. The basic two fluid model (Appendix I) predicts no interaction between superfluid and normal fluid for flow velocities below many meters per second (14). The airfoil would on this model be expected to exhibit zero lift up to free stream velocities of at least several meters per second (assuming the edges of the wings to be smoothly rounded (see Part III.2c). The observed superfluid velocities of several cm/sec or less for the onset of lift are in conflict with this model. The nonappearance of lift for lower velocities indicates that in this range the two fluid model remains valid.

Several theories may be relevant to an understanding of the experimental results obtained. None of these have thus far been successful in providing an explanation of the observations. In this section we analyze the behavior of airfoils in classical fluids and then discuss several unsuccessful but interesting theoretical approaches.

In Part III.1 we summarize the classical results for an elliptical airfoil. The Kutta-Joukowski theorem relating the circulation about an object to the lift forces is presented, as are the equations relating the local velocity about an elliptical airfoil with arbitrary circulation to the free stream velocity.

Part III.2 presents several modifications of the classical lift laws based upon changes in the boundary conditions. One of these modifications leads to the functional form $\tau = a\nu(v-v_c)$ used in presenting the experimental data, but since the coefficients predicted by the

theory differ by a factor of up to ten from those observed, the theory cannot be considered successful.

Part III.3 discusses the application of a quantum mechanical analysis to the operation of the airfoil. The theory predicts that lift will appear in discreet steps rather than continuously, as observed. The failure of the theory to describe the observations may be attributed to the presence of noise. A decision as to the validity of this theory cannot be made on the basis of this experiment.

III.1 SUMMARY OF CLASSICAL LIFT THEORY

The significance of the results in the "superfluid wind tunnel" may be assessed in the light of classical airfoil theory. We therefore summarize the basic classical results.

The study of forces acting on a body placed in a moving fluid has been of interest for many centuries. The first quantitative investigation of drag forces was a study by Alembert (1) in 1752 of the drag on a sphere placed in a stream. His theoretical conclusion that the drag should vanish was in direct contradiction to his experiments, and became known as Alembert's paradox. The situation was not resolved until it was realized much later that viscous forces, which had been neglected in his theory, were of fundamental importance in determining both lift and drag.

The first quantitative investigation of lift forces was performed by Newton, who "proved" by means of a momentum analysis of the forces acting on a flat plate that flight was impossible. His arguments, based on an individual particle model of air, led to a lift law which is said to have held back the development of flight for a century. Today this law finds application in the theory of supersonic flight.

a) Kutta-Joukowski theorem

Full understanding of the mechanism responsible for lift began with Lord Rayleigh's investigations concerning the flight of tennis balls. The effect involved (Magnus effect) may be treated by considering the two dimensional situation where an infinite cylinder of arbitrary cross section is placed perpendicular to a velocity field

uniform at infinity. Any circulation about the object may be shown to give rise to a lift force normal to the free stream velocity and the cylinder axis (Kutta-Joukowski theorem) (Appendix II). The force is

$$L = \rho v C \qquad \text{dynes/ unit length} \qquad (7)$$

where (ρ) is the fluid density in gm/cc, (v) the free stream velocity in cm/sec and (C) the circulation defined by $C = \oint \bar{v} \cdot d\bar{l}$. The path of integration can be any clockwise route surrounding the object. For nonviscous flow the drag force vanishes, regardless of the amount of circulation (C) that may be present.

b) Effect of viscosity

A knowledge of the free stream velocity and the circulation is sufficient for determining the lift force on any object. However, the magnitude of the circulation is not immediately evident. In fact, in the absence of dissipative forces the circulation cannot change, for no mechanism exists to change the system energy. Should a nondissipative system possess no circulation at a particular instant the circulation must remain zero at any succeeding time, and therefore the system can never show lift (Kelvin's circulation theorem (13)).

The part which viscosity plays in determining the fluid flow may be seen by looking at the hydrodynamical equations of motion. The fundamental equation of hydrodynamics is the Stokes-Navier equation for a viscous fluid:

$$\rho \frac{d\bar{v}}{dt} = -\nabla P + \eta \nabla^2 \bar{v} \qquad (8)$$

where (p) is the pressure in dynes/cm^2 and (η) the viscosity in gm/cm-sec. The boundary conditions to be used with this equation are the vanishing of the normal and tangential components of velocity at

any surface. However, for zero viscosity the equation reduces to

$$\rho \frac{d\bar{v}}{dt} = -\nabla P$$

which is of lower order. Thus a perfect fluid cannot be expected to obey all the boundary conditions of a real fluid. The boundary condition of zero tangential velocity is lost, and the fluid may slide along the walls. The flow pattern in the limit as $\eta \to 0$ may be completely different from that obtained if $\eta \equiv 0$. This result is in fact observed in superfluid helium II.

The importance of viscosity in a particular situation may be estimated by looking at the ratio of acceleration forces to viscous forces in equation 8:

$$\left[\frac{\rho \frac{dv}{dt}}{\eta \nabla^2 v} \right] = \left[\frac{\rho v d}{\eta} \right] = Re$$

Here (d) is some characteristic length associated with the apparatus and the dimensionless quantity (Re), called the Reynolds number, is the fundamental parameter determining the flow character. Similar solutions to geometrically similar hydrodynamical problems are obtained for equal Reynolds numbers independent of the fluid involved.

c) Kutta condition

Thus far we have not specified how the circulation about a body shall be determined. For an arbitrary shape the problem cannot be solved theoretically. However, Kutta and Joukowski pointed out independently that for a wing with a sharp trailing edge, dissipation effects must be maximal where the local velocities are highest and the shear forces therefore maximum, and that this will occur at the trailing edge. The boundary condition in such a case then requires that the local velocity

at the trailing edge vanish. This condition, usually known as the Kutta condition, does not depend in any way upon the magnitude of the viscosity, but only upon its existence (fig. 11).

d) Classical lift on an elliptical cylinder

We can apply the condition to a practical example, the two-dimensional problem of a wing of elliptic cross section and infinite span inclined at an angle (γ) to a flow uniform at infinity. The local tangential velocities with arbitrary circulation may be found at various locations on the wing (Appendix III):

$$\text{Front} \quad v_f' = C/(\pi n) + v(1 + w/n) \sin\gamma \tag{9a}$$

$$\text{rear} \quad v_r' = C/(\pi n) - v(1 + w/n) \sin\gamma \tag{9b}$$

$$\text{top} \quad v_t' = C/(\pi w) + v(1 + n/w) \cos\gamma \tag{9c}$$

$$\text{bottom} \quad v_b' = C/(\pi w) - v(1 + n/w) \cos\gamma \tag{9d}$$

where

v = free stream velocity at infinity
w = major axis of the ellipse (wing chord)
n = minor axis of ellipse (wing thickness)
γ = angle of attack ellipse makes with the free stream velocity

C = circulation = $\oint \bar{v} \cdot d\bar{l}$

Primed velocities are local while unprimed velocities are to be measured at infinity. Thus a velocity (v_f) at infinity creates a local velocity (v_f') at the front edge of the ellipse.

The Kutta condition demands that the local velocity vanish at the trailing edge ($v_r' = 0$, equation 9b). This determines the circulation to be

$$C = \pi(n+w)v \sin\gamma$$

The lift per unit length is found from equation 7 to be

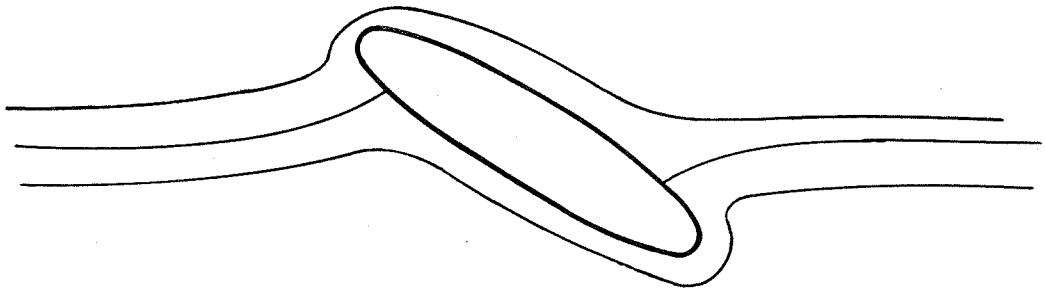

ELLIPTICAL WING WITHOUT CIRCULATION

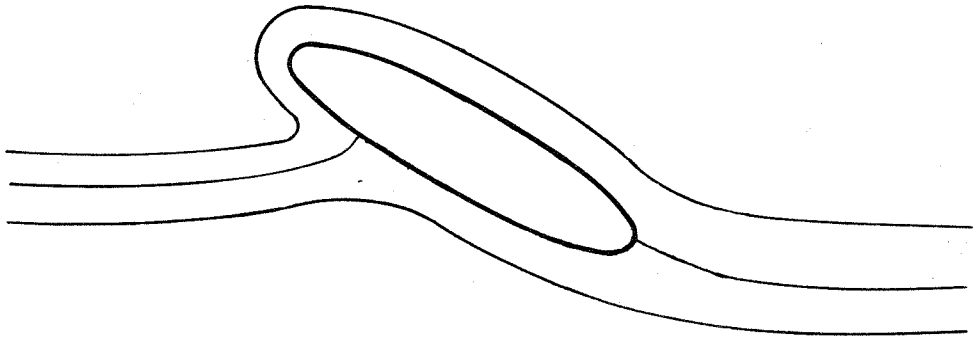

ELLIPTICAL WING WITH KUTTA CONDITION SATISFIED

FLOW ABOUT AN ELLIPTICAL WING

FIGURE 11

$$L = \rho v C = \pi \rho (n+w) (\sin \gamma) v^2 \text{ dynes/unit length} \qquad (10)$$

For a thin wing ($n \ll w$) making a small angle of attack ($\sin\gamma \sim \gamma$) we obtain

$$L = (2\pi\gamma) w (\tfrac{1}{2}\rho v^2) = C_L w (\tfrac{1}{2}\rho v^2) = A \rho v^2 \text{ dynes/unit length} \qquad (11)$$

Here the classical lift coefficient ($C_L = 2\pi\gamma$) and the lift factor ($A = \pi w \gamma$) have been introduced.

e) Finite wing

The discussion has thus far been confined to two dimensional flow over a wing of infinite span. The case of a wing of finite span is far more difficult. The lift distribution across the span of experimental wings approximates in most cases a parabola, with maximum lift at the wing center and zero lift at the tips. Any nonconstant distribution produces a downwash velocity with an attendant induced drag. The parabolic distribution provides the smallest induced drag consistant with the condition of zero lift at the wing tips. The effect upon the infinite wing equation may be expressed by introducing an effective attack angle

$$\gamma_{eff} = \gamma/(1 + 2/AR)$$

where the aspect ratio (AR) equals the span squared divided by the wing area (S)(cm^2). The total lift force (F) on the wing now becomes

$$F = \frac{2}{(1 + 2/AR)} (\tfrac{1}{2}\rho v^2) S \quad \text{dynes}$$

f) Air calibration

A finite wing placed in a wind tunnel, the dimensions of which are comparable to those of the wing, shows a lift factor lying between that of the infinite wing and the finite wing. In the present experiments the aspect ratio was usually sufficiently large that the

difference between these two limits was small. The results of air calibration usually fell between the limits. In any case an effective lift factor (A') could be determined experimentally which usually satisfied the inequality $A/(1 + 2/AR) \leqslant A' \leqslant A$. The quantity (A') proves useful in the interpretation of results (see Part III.2).

g) Stall point

The thin wing formula has been experimentally investigated by Wick (20) as a function of attack angle. He finds that the classical lift coefficient predicts the observations well for attack angles below 8°, above which the wing stalls and the observed lift drops to a low value (fig. 12). The effect may be qualitatively understood in terms of the flow pattern. With no circulation about a symmetrical wing the local velocity should be the same at the leading and trailing edges. Flow studies in wind tunnels show that well below the stall angle the flow separates from the front edge of the wing and reattaches a short distance back. The reattachment point moves back as the attack angle increases until eventually at the stall point reattachment fails to occur at all. The character of the flow changes abruptly, and the thin wing lift formula we have discussed no longer applies.

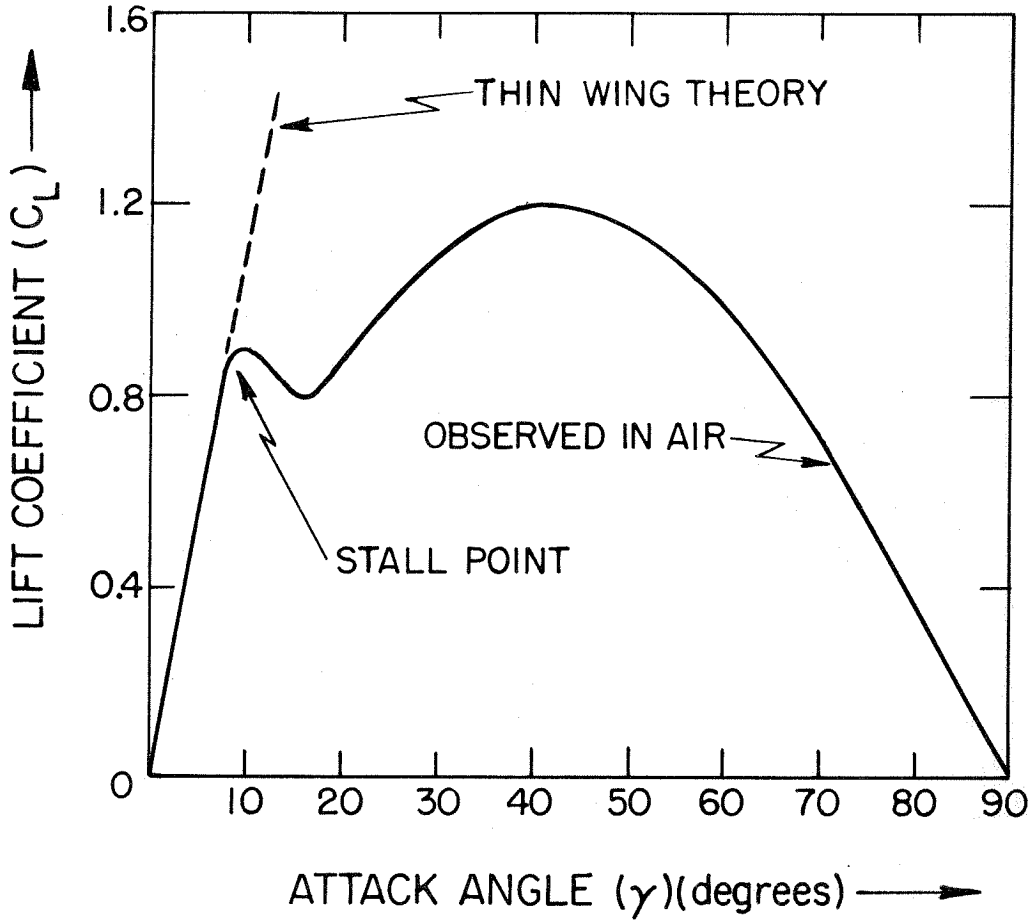

CLASSICAL EXPERIMENTAL VARIATION OF LIFT COEFFICIENT (C_L) WITH ATTACK ANGLE (γ) (WICK (20))

FIGURE 12

III.2 MODIFIED CLASSICAL THEORY

We summarize the basic observations on an airfoil placed in a flow of superfluid helium II. For velocities below some (temperature dependent) critical velocity the lift force exerted by the superfluid lies at least two orders of magnitude below that exerted by a classical fluid of the same density, and may possibly vanish. This result shows that the circulation about the airfoil remains approximately zero, and that the classical Kutta boundary condition of zero tangential velocity at the trailing edge of the wing no longer applies. We may interpret this as implying the conclusion that the viscosity term in the Stokes-Navier equation vanishes identically, for even in the limit as the viscosity approaches zero the Kutta condition would be expected to obtain. A further implication must then be that superfluid helium is capable of undergoing pure potential flow without dissipation.

a) Modification of the Kutta condition

When the maximum local velocity at the airfoil exceeds some critical value (v_c') corresponding to a free stream velocity (v) a dissipative mechanism begins to operate. It is not clear what form this mechanism should take, but in any event circulation appears about the wing producing lift. Since the classical Kutta condition assumes that dissipation is most important at the trailing edge, we suppose that also in this case dissipative effects commence there. As circulation appears the local trailing edge velocity will be reduced. It evidently cannot drop below (v_c') since in that case the dissipation mechanism would become inoperative, thus precluding further circulation. The first possibility for a lift law is embodied in the

assumption that the local trailing edge velocity must be maintained at the threshold value (v_c') if the free stream velocity exceeds (v_c).

Setting $v_r' = -v_c'$ in equation 9b we find the circulation about an infinite elliptical wing of thickness (n) and chord (w) to be:

$$C = \pi n \left[(1+w/n)\, v \sin\gamma - v_c' \right] \tag{12}$$

so that the lift (equation 7) for the present case becomes, using now the superfluid density (ρ_s),

$$L = \rho_s v C = \pi n \rho_s v \left[(1+v/n)\, v \sin\gamma - v_c' \right] \tag{13}$$

We can relate the local critical velocity (v_c') to the free stream velocity (v_c):

$$v_c = \frac{v_c'}{(1+w/n)\sin\gamma} \tag{14}$$

Then, in the limit $n \ll w$ and $\sin\gamma \sim \gamma$, the lift reduces to:

$$L = 2\pi\gamma(\tfrac{1}{2}w)\rho_s v^2(1-v_c/v) \qquad v \geq v_c$$

It proves convenient to express this quantity in the modified forms:

$$\begin{aligned} L &= wC_L(\tfrac{1}{2}\rho_s v^2)(1-v_c/v) && v \geq v_c \\ &= L_{classical}(1-v_c/v) && v \geq v_c \end{aligned} \tag{15}$$

and

$$L = A\rho_s v(v-v_c) \qquad v \geq v_c \tag{16}$$

In the preceding we have used the lift factor $A = (2\pi\gamma)(\tfrac{1}{2}w)$, the classical lift coefficient $C_L = 2\pi\gamma$, and the classical lift $L_{classical} = C_L\, w(\tfrac{1}{2}\rho_s v^2)$ (see Part III.1d). Equations 15 and 16 represent modifications of the Kutta boundary condition in which the local trailing edge velocity may never exceed the threshold value (v_c').

Qualitatively equation 16 may be understood by considering the local trailing edge velocity as composed of the difference between a contribution proportional to the free stream velocity alone (pure potential flow) and a contribution proportional to the circulation velocity. By setting the circulation velocity (and hence the circulation) proportional to the difference between the free stream velocity and the critical velocity, we in effect require the local velocity at the trailing edge of the wing to remain constant (and unequal to zero). Since the Kutta-Joukowski theorem (equation 7) places lift proportional to the product of the free stream velocity times the circulation, we obtain (in contrast to the classical case) a lift proportional to the product of the free stream velocity times the difference between the free stream and critical velocities.

As might be expected, this result approaches the classical expression in the high velocity limit (the second term in parentheses in equation 15 becomes negligible). A modification of equation 16, with (A) replaced by a new parameter (m), becomes the fundamental equation for expressing the experimental results.

b) Analysis of data using the modified Kutta condition

The experimental results may be analyzed in terms of this modification of the Kutta condition. In so doing we emphasize the qualitative arguments leading to equation 16 and treat the equation as a semi-empirical functional form derived for describing the experimental results. The parameters (A) and (v_c) are now determined experimentally. To emphasize this point we replace (A) by an entirely new parameter (m), and write

$$L_{observed} = m\rho_s v(v-v_c) \qquad v \geqslant v_c \qquad (17)$$

where (m) and (v_c) are to be chosen for optimal fit to the data. At any fixed temperature, (m) and (v_c) may be determined by plotting ($L_{observed}/(\rho_s v)$ versus (v)). In all cases the observations lie closely on a straight line, from which (m) may be directly obtained as the slope and (v_c) as the axis intersection. In order to connect this analysis to the representation of the experimental data of Part II.1, we must relate the lift per unit length on an airfoil to the torque on the wing assembly. The total lift force on the airfoil is obtained by multiplying equation 17 by the wing span (r). Multiplication by the mean spacing (r') of the wing center from the pivot point yields the torque on the system. In the experiments performed (r') was approximately half of (r). The torque then becomes

$$\tau = m\rho_s v(v-v_c)rr' \sim \tfrac{1}{2}m\rho_s r^2 v(v-v_c) \qquad (17a)$$

Comparison of equations 6 and 17a shows that $m \sim 2a/\rho_s r^2$. Thus the lift factor (m) may be determined from the data of Table 1.

Comparison of this theory with experiment may be accomplished by comparing the experimental lift factor (m) with the classical lift factor (A') determined by air calibration and discussed in section III.2. This is equivalent to comparing columns (14) and (11) of Table 1. The theory predicts the ratio of these factors to equal unity for each wing. Observed values vary from 0.135 (wing #6) to 0.56 (wing #4). As the prediction of this quantity constitutes a crucial test for the theory we must conclude that the theory as presented here proves inadequate to deal with the experimental results.

c) Estimate of local critical velocities

The local velocity at which dissipative effects begin to appear can be estimated in terms of the free stream velocity by assuming the wing to be elliptical in cross section and using equation 9b with the circulation set equal to zero. The local velocity at the trailing edge is given by $v_r' = v(1 + w/n)(\sin\gamma)$ for a wing of chord (w) and thickness (n).

For example, if we assume wing #2 (Table 1) to be elliptical in cross section the local trailing edge velocity exceeds the free stream velocity by a factor of about 1.8. The free stream critical velocity (v_c) of 6.5 mm/sec then implies a maximum local velocity at the trailing edge of 1.17 mm/sec. This figure certainly has little significance as the wing is far from elliptical.

Possibly the maximum local velocity occurs in some region other than the trailing edge such as at the wing top. The local wing top velocity without circulation, $v_t' = (1 + n/w)\cos\gamma v$ (equation 9c) exceeds that at the trailing edge if $\tan\gamma < (n/w)$, i.e., for small attack angles or thick wings. This situation occurs in some of the wings investigated under the assumption that they are truely elliptical with major axis (w) and minor axis (n). In practice the trailing edges tended to be quite sharp, so we suppose in deriving all equations that dissipation always begins to appear first at the trailing edge.

d) Correspondence principle

The preceding formulation, which has been found to represent the experimental results semi-empirically (Part II), was based on the assumption of a fixed local critical velocity (v_c') above which

superfluid flow breaks down. Clearly this requirement could constitute an over-restriction, and a more generalized approach may prove appropriate. For this purpose an attempt has been made to apply a correspondence principle to the problem.

Correspondence principles which have been proposed are often of the form

$$v_a y^{1/s} = \text{constant} \tag{18}$$

where (v_a) and (y) represent respectively a velocity and a distance related to the experiment. The constant may be a function of temperature, and (s) (usually an integer) is predicted by the particular theory. In order to apply such a principle to the present experiment we suppose that the local critical velocity need no longer remain constant (equal to the threshold value (v_c')) but must be related by the principle to some suitable distance associated with the experiment.

For a free stream velocity (v_c) greater than the local critical velocity (v_c') the circulation must, as before, increase so long as dissipative forces continue to act. As a result the stagnation point, located on top of the airfoil in the absence of circulation (fig. 11), moves closer to the trailing edge. There is thus created a variable distance between the stagnation point and the trailing edge which is related to the circulation and hence to the local trailing edge velocity. This distance and velocity might reasonably enter into the correspondence principle. The circulation cannot as before be proportional to ($v-v_c$), but rather must be adjusted to satisfy the functional relationship specified by the correspondence principle between the trailing edge velocity and the location of the stagnation point.

This analysis when applied to the Kutta-Joukowski theorem (equation 7) leads to a new form for the lift law (Appendix IV) which may be expressed in a manner analogous to equation 15 as a modification to the classical lift law:

$$L = L_{classical} \quad 1 - (v_c/v)^{s/(s+1)} \qquad v \geq v_c \qquad (19)$$

$$L = 0 \qquad v \leq v_c$$

The velocity and distance introduced in equation 18 have been eliminated from this equation by expressing the result in terms of the experimentally observable free stream critical velocity (v_c) (the velocity corresponding to the onset of lift). Equation 19 vanishes at $v = v_c$ and approaches the classical limit at high velocities.

In the limit as $s \rightarrow \infty$ the correspondence principle (equation 18) reduces to v_a = constant, and equation 19 simplifies to the special case presented in part a) (equation 15) above. Setting $s = 2$ we obtain the lift law implied by a correspondence principle proposed by Dash (4) and others (6), while with $s = 1$ we find the lift law implied by Feynman's correspondence principle (8) (Appendix 1).

e) Analysis of data using the correspondence principle

Data may be analyzed using the lift law derived from the correspondence principles in much the same manner as for the law derived from the modified Kutta condition (b) above. Equation 19 may be written with adjustable parameters (m_s) and (v_c) as

$$L = m_s \rho_s v^2 (1 - (v_c/v)^{s/(s+1)}) \qquad v \geq v_c \qquad (19a)$$

where (m_s) denotes a parameter (m_1) for $s = 1$ and a parameter (m_2) for $s = 2$. The values of (m_s) and (v_c) are chosen to obtain the best fit to the experimental data.

The form of equation 19a does not lend itself to the simple curve fitting process in section b) above. Fortunately another approach may be used. Within the velocity range $1.5\ v_c < v < 3v_c$ the ratio of the lift laws implied by the correspondence principles for $s = 1$ and $s = 2$ to the law obtained by the modification of the Kutta condition are constant to within about 6%. For the entire range $v_c < v < 3v_c$, the experimental data are inadequate for distinguishing between the shapes of the three lift curves.

It may be shown (Appendix IV) that for $s = 2$, (equation 19/equation 15)$_{(s = 2)} = (1-(v_c/v)^{2/3})/(1-v_c/v) = 0.74 \pm 0.04$; and that for $s = 1$, (equation 19/equation 15)$_{(s = 1)} = (1-(v_c/v)^{1/2})/(1-v_c/v) = 0.59 \pm 0.04$ so long as $1.5v_c < v < 3v_c$.

Therefore, once a value for (m) has been obtained using equation 15, the values of (m_1) and (m_2) to be used in equation 19a follow immediately:

$$m_2 = (1/0.74)m = 1.35\ m \qquad s = 2$$

$$m_1 = (1/0.59)m = 1.70\ m \qquad s = 1$$

By means of this device the lift laws derived from the correspondence principles may be fitted to the experimental data without further computation. The same value of (v_c) applies in all cases.

Using the conclusions arrived at in b) above, we find that the quantity (m_2) varied from 18% (wing #6) to 75% (wing #4) of the value predicted by the theory, while (m_1) varies from 23% to 95% of the predicted value.

Since the theory purports to predict the constants (m_1) and (m_2) in terms of the system geometry, and the observed values fail by

a large margin to agree with the calculated values, we must conclude that although this theory is more satisfactory than that of section a) above it too proves inadequate.

f) Conclusions

The discussions of this section are not adequate to describe the results experimentally obtained. Consequently they must be considered as purely heuristic, finding what usefulness they may possess in their ability to justify a convenient means for representing the experimental results. There has appeared no useage of the quantum mechanical aspects of helium, except through the recognition of the two fluid model. The failure of more sophisticated analyses to describe the observations provides justificationfor the inclusion of this approach. In the following section we discuss one promising quantum mechanical analysis of the experiment.

III.3 QUANTUM MECHANICAL THEORY AND THE NONAPPEARANCE OF VORTEX LINES

The basic motivation for this experiment may be found in the two fluid model of helium II. As originally envisaged by Professor Pellam, an investigation into the lift forces exerted on an airfoil placed in a flow of pure superfluid helium could provide powerful evidence for the identical vanishing of viscosity within the superfluid component. This proposal was advanced prior to the existence of Feynman's detailed quantum mechanical theory of the rotation of helium II (8).

Early in the investigation, after the original apparatus had been assembled, Professor Feynman made two quantum mechanical analyses of the experiment, leading to predictions for the behavior of the apparatus. The first of these suggested that the lift observed should follow the classical behavior for an airfoil in a viscous fluid of high Reynolds number. The experimental data of Part II show that this does not occur, but rather the lift lies orders of magnitude below that expected classically.

After it had been established experimentally that superfluid exerted zero lift at small flow velocities followed by positive lift at higher velocities, it was proposed by Feynman that in the range where lift appeared, it should develop in discontinuous quantized steps. In this section we discuss the theory behind such a proposal and the factors which may have been responsible for the failure of the effect to appear.

a) Predicted results

Onsager (15) and Feynman (8) have independently proposed the existence of quantized vortex elements within helium II. Feynman has

suggested that the experiment might reveal the existence of discrete, quantized circulation about an airfoil placed in a flow of pure superfluid. He proposed that the circulation (C) might appear in integral multiples of the ratio of Planck's constant (h) to the mass of the helium atom (m). Thus $C = \oint \bar{v} \cdot d\bar{l} = 2\pi(\hbar/m)n$ where (n) is an integer and ($\hbar$) is Planck's constant divided by (2π) (Appendix I, equation 24). The lift per unit length on an airfoil then becomes (using the Kutta-Joukowski theorem (Part III.1, equation 7)) $L = \rho v C = 2\pi(\hbar/m)\rho nv$ dynes/cm, independent of the wing span and attack angle.

A graph of lift force versus velocity for an airfoil placed in a flow of pure superfluid helium II should then consist of a straight line section for each (n), where each segment projects through the origin. There exists at present no way to estimate the factors which determine (n), nor for what velocity range a given value of (n) might obtain. However, observations would not be expected to lie in regions corresponding to non-integral values for (n) unless it should occur that circulation does not appear about the entire wing simultaneously (see d) below).

b) Experimental details

Approximately one year was spent in an unrewarded effort to detect this effect. By choosing an airfoil which exhibited zero lift up to a reasonably high velocity, and using a sufficiently fine fiber suspension, the apparatus was rendered capable of detecting changes in lift corresponding to the appearance of just one unit of circulation. Thus in (fig. 8) the torque expected from the presence of one unit of circulation about each wing would be described by the line

$\tau = 0.013$ v millidyne, which passes through $\tau = 0.08$ millidynes at a velocity of 6 mm/sec, and should be easily observable. The resolution of the apparatus was such that at a velocity of 6 mm/sec a change in torque corresponding to the appearance of only one tenth of a unit of circulation could be observed. Experimental observations showed the onset of lift to be in all cases continuous (i.e., not describable by integral values of (n)). There was no evidence whatever for discrete changes in the observed lift, as predicted by the theory, nor was there any evidence for hysteresis, which would be expected if a line of circulation could remain attached to the wing assembly as the superfluid velocity was reduced.

The failure of discrete changes in lift to appear cannot be construed as a conclusive demonstration of the inapplicability of the vortex theory to the present experiment. Experimentally observed instability of the wing assemblies within the test sections proved a major obstacle to an unequivocal conclusion. For an undamped wing assembly irremovable random oscillations were of the same order of magnitude as the changes in lift expected. In all cases these oscillations had a characteristic frequency roughly equal to that of the undamped wing assembly, and amplitudes corresponding to changes in (n) of from one to ten or more units (the amplitude of the oscillations increased with superfluid velocity). Investigation of the average time spent by the wing assembly at a given deflection (for fixed superfluid velocity) demonstrated there was no observable tendency toward stability at particular angles as might be expected should the circulation have a preference for specific values. That these oscillations are probably

due to non-quantum-mechanical irregularities in the fluid flow or to instability of the wing assemblies and are not an intrinsic feature of superfluid is evidenced by their appearance in a wind tunnel utilizing the normal fluid component of helium II (Part I.3). That the amplitudes of the oscillations are of the same order of magnitude as the quantization effects under study is probably fortuitous.

For experimental purposes a damping device (Part I.2) served virtually to eliminate observation of these effects. However the mechanism responsible for the oscillations remains present, and could well cause the quantized circulation elements to attach and detach from the wing at random, or to attach to only a part of the wing. Such behavior could lead to an averaging process which would obscure the discrete changes predicted by the theory.

Should the quantized circulation lines for some reason fail to attach to the entire wing, the magnitude of the jumps would be unknown. Conceivably the lines are intrinsically unstable on a large airfoil, and the noise effects within the apparatus do not constitute the principle difficulty. However, the reduction of the noise must constitute the first step in further work on the problem.

It should be emphasized that the original motivation for constructing the apparatus was the possibility of observing pure potential flow without dissipation. This result was rather strikingly implied by the observations (evidenced by the data of fig. 7). The investigation of quantization represents an attempt to ellicit performance from the apparatus for which it was not originally designed.

c) Theory

The expectation of the appearance of such quantized lift effects may be understood in terms of the Bose-Einstein statistics obeyed by He^4 nuclei. Feynman has shown (8) that a wave function capable of describing the excitation spectrum of helium II is curl free. That is, it is incapable of supporting circulation (Appendix I). Thus helium II placed in a situation where forced to undergo circulation must do so in a manner unlike that of any other fluid.

Circulation instead of being continuously distributed throughout the liquid must, in order that the liquid possess minimum energy, be concentrated in highly localized regions. In a state of rotation helium II should contain excitation lines or vortex lines about which circulation exists, and between which lie circulation free regions. Because the wave function must be single valued the magnitude of circulation about each vortex line must be quantized in units of (h/m).

In a multiply connected region the situation may be somewhat different, for circulation can exist within the total region while each local region remains circulation free. The requirement of single-valuedness for the wave function remains, so even in a macroscopic multiply connected region circulation would be expected to be quantized. Thus a macroscopic mass of helium II would be enabled to move in an ordered fashion, and Planck's constant would be exhibited on a macroscopic scale.

d) Shortcomings of the theory

There exist no predictions as to the stability of such configurations. It is not implausible that only in an extremely smooth flow situation could a given value of circulation obtain for long periods

of time. Thus an experiment capable of detection of the effect might require extreme uniformity of flow and lack of vibration. The noise and oscillation effects within the present experiment suggest that the difficulties encountered may stem from this cause.

Further, the theory fails to predict whether circulation prefers to lie along the path of an object (along the span of an airfoil) or might rather detach at some intermediary point and move into the main fluid flow. Thus a demonstration of the proposed discrete steps would provide powerful evidence for the validity of the concept of circulation quantization, but their nonappearance may indicate only that the apparatus is insufficiently stable.

e) Discussion

In the light of this theory there are a number of difficulties which arise in the interpretation of the data. For example with wing #1 virtually no lift force is observed for velocities below 6 mm/sec (fig. 7). At this velocity about 120 lines would have to be present to yield the classically expected lift. There exists at present no explanation for the failure of circulation to develop at such high velocities, even though this would appear energetically desirable. Within experimental accuracy no hysteresis effects have been observed whatever. Even should lines form on only a part of an airfoil so that the jumps would be immeasurably small, it would be plausible to suppose that hysteresis effects might appear as the velocity is increased and decreased. The only present suggestion for the failure of hysteresis to occur is based upon the large amounts of noise in the apparatus, due probably to irregular flow, which could cause circulation to appear and disappear rapidly.

The observed lift shows no tendency to approach the classical value over the range of velocities investigated. The torques observed are less than those expected classically by at least two orders of magnitude for the lowest velocities, and by a smaller but appreciable amount at higher velocities. Feynman has considered the possibility that the observed lift may be due to a mechanism entirely divorced from circulation. The similarity between the results displayed in (fig. 7) and classical results in media of high viscosity led him to notice that in some sense superfluid helium might be behaving in this experiment as though it possessed an extremely great viscosity. The failure of the airfoil to develop appreciable lift up to quite high velocities of flow and the failure to approach the classical value possibly constitute the greatest challenge to theory offered by the experiment.

IV COMPARISON WITH OTHER EXPERIMENTS

The present experiment demonstrates that the lift exerted by the superfluid component of helium II lies (for the range of velocities investigated) far below that expected classically. At low velocities the observed lift has been shown to be at least two orders of magnitude below the classical value. When lift first occurs, it sets in with extreme rapidity. These results suggest that circulation may be completely absent at low flow velocities, and the flow observed be pure potential flow without dissipation. This result agrees with several previous experiments.

Kapitza (11) in 1941 performed an experiment wherein he investigated the reaction forces of helium jets upon flat plates immersed in helium II. He discovered that the reaction force exerted by normal fluid far exceeded that of superfluid, showing that dissipative effects within normal fluid greatly exceed those within superfluid. His experiment demonstrated only a difference effect and failed to indicate that the superfluid flow was indeed dissipation free.

A recent experiment by Hall (9) has demonstrated the possibility of persistent currents of helium II analogous to persistent currents in superconductors. By measuring the angular momentum contained in a system of rotating Andronikashvili type disks he was able to show the existence of stored angular momentum for times long compared to the relaxation time of the normal fluid. Persistent currents lasting as long as twenty minutes were obtained.

Hollis-Hallett (10) has measured charges in period and damping decrement as the amplitude of oscillation of disks suspended from torsion

fibers in helium II baths is increased. He finds that above some critical amplitude the damping decrement undergoes a discrete change in slope. The maximum peripheral velocity of the disk corresponding to the amplitude where nonlinearity first appears might be related to a local critical velocity. Such an analysis of the experiments has been attempted by Dash (4). However, Dash's interpretation of the data as implying a critical velocity may be questioned, for this analysis is not consistent with Hollis-Hallett's data for various sizes of disks. It is at least certain that some type of nonlinearity exists which may be related to a local velocity.

A variety of capillary flow experiments have indicated the existence of pure potential flow. Those of Winkel et al. (21) are representative. Measurement of flow resistance as helium II is pressed through fine capillaries indicates small resistance to flow at low velocities, with a discrete onset of high resistance at some critical velocity. The critical velocity may be related to the capillary dimentions by a correspondence principle of the type used in Part III.2, i.e., the product of the critical velocity times a characteristic dimension raised to some power is constant. The order of magnitude of the critical velocity obtained from such experiments would not be expected necessarily to correspond to that found in the present experiment. However, the temperature dependence of the critical velocity might be comparable.

In (fig. 13) we plot a critical velocity obtained in the present experiment (data of fig. 10) versus temperature. Also presented are the results of Hollis-Hallett (10) as given by Dash (4) and some representative

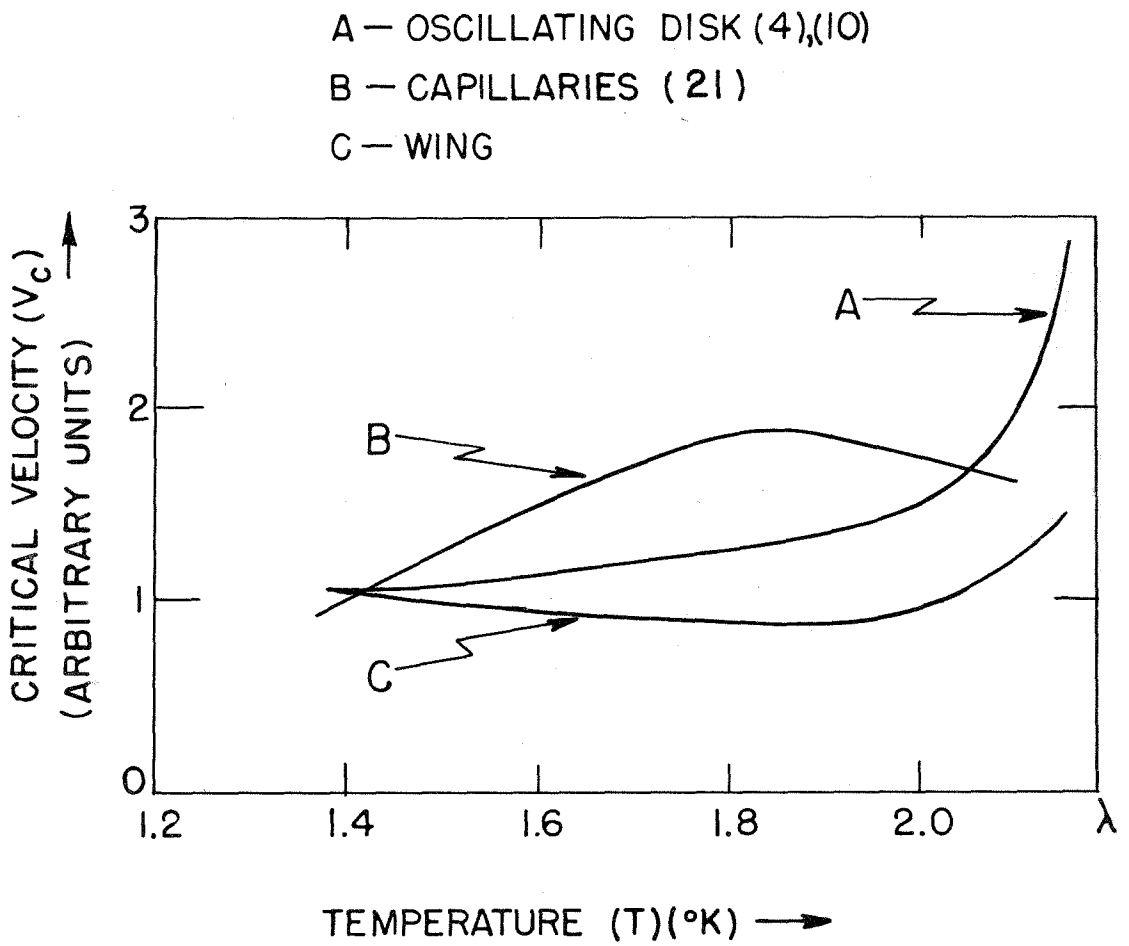

COMPARISON OF EXPERIMENTS YIELDING CRITICAL VELOCITIES (NORMALIZED FOR AGREEMENT AT $T = 1.4°K$)

FIGURE 13

results of Winkel (21). The data have been normalized to agree at T = 1.4°K for comparison purposes. This was done since the numerical value of the velocities is felt to be not so significant as the temperature dependence.

The behavior in the neighborhood of the lambda point constitutes the most striking aspect of (fig. 13), for the critical velocity obtained in the oscillating disk experiment and in the present experiment rises near the lambda point, whereas that obtained from capillaries falls. This phenomenon suggests some basic difference between experiments performed in open vessels and those performed in enclosed regions. There exists no theoretical reason for this behavior.

V CONCLUSIONS

For sufficiently low velocities an airfoil placed in a flow of pure superfluid helium II fails to develop lift, i.e., the classical lift expected exceeds the observed lift by at least two orders of magnitude. This indicates that the viscosity of the superfluid component vanishes identically. The flow obtained is probably pure potential flow without dissipation.

Upon detailed examination of the zero lift region a slight apparently negative lift can be detected which has not been quantitatively accounted for but which may possibly be attributed to reverse leakage of normal fluid within the apparatus. At higher velocities positive lift appears. The results in the high velocity range can be described by an equation of the form $L = m\rho_s v(v-v_c)$ where (L) is the observed lift/unit length on the wing system, (m) is a temperature and geometry dependent parameter, and (v_c) is the velocity at which lift first appears. The variation of (m) with temperature has not been investigated. The variation of (v_c) with temperature has no theoretical explanation. The critical velocity increases at both the low temperature limit and near the lambda point, having a minimum at about 1.95°K where the superfluid and normal fluid densitites are approximately equal. The rise near the lambda point agrees qualitatively with the results of oscillating disk experimental results. The low temperature results disagree with both oscillating disk and capillary data.

The "superfluid wind tunnel" used in the experiment provides a separated velocity field wherein the normal fluid component of helium II is immobilized while the superfluid component can flow. It offers a

unique tool for the investigation of a variety of classical hydrodynamical results for perfect fluids. The low velocity outcome of these experiments is not in doubt, for the wing experiments are about as stringent demonstrations of the nonexistence of viscosity as can be found. Still, direct verification would be satisfying. At higher velocities when pure potential flow breaks down anomalous results must certainly appear. These may serve to enlighten the subject of break-down phenomena.

The investigation of drag on a sphere placed in pure potential flow has been suggested as a possible experiment along these lines. Because the geometry can be accurately controlled, it should be possible to characterize explicitly the conditions for the onset of dissipation. Classically drag depends upon the Reynolds number of the flow. In superfluid some correspondence principle might replace the Reynolds number as a means of comparing similar experiments.

Classically a cylinder placed in a uniform flow sheds alternating vortices at a characteristic rate. The frequency (f) may be found (13) to be $f = (v/a)$ (function of Re) for a cylinder of radius (a) in a stream of undisturbed velocity(v). Classically the function of Reynolds number is determined experimentally and known as the Strouhal number. The vortices show up as pressure fluctuations which could be detected by a suitable sensing device such as a capacitance or crystal microphone.

The general subject of breakdown of superfluid flow in macroscopic regions would appear to be fruitful. The fundamental qualitative differences between capillary results and those in open regions should be investigated and clarified.

APPENDIX I

SUMMARY OF HELIUM THEORY AND THE TWO FLUID MODEL

More than a quarter century elapsed between Kamerlingh Onnes' liquifaction of helium and the first realization that quantum mechanical effects were intimately connected with the phenomena observed. Classical concepts proved inadequate to explain the phenomena observed. The first such suggestion was by Simon (17) in 1934. He proposed a modification of Trouton's rule which states that the latent heat of vaporization (L) (cal/mole) divided by the condensation temperature (T) is constant and equal to 22 calories/mole-degree. This rule was known to work well for heavy gases but to break down badly for the light gases. Simon's proposal was that the low latent heat of the light gases might be caused by a large zero point energy. He therefore modified Trouton's rule to include a zero point term (E_o)

$$(L-E_o)/T = \text{const} = 21 \text{ cal/mole deg}$$

The zero point energy of helium is then found to be 64 cal/mole using the observed latent heat of 22 cal/mole. This very high zero point energy was suggested as an explanation for the low density of liquid helium (0.145 gm/cc) as well as its failure to solidify under its own vapor pressure.

a) Bose-Einstein condensation

Following suggestions of this nature F. London proposed in 1938 that the properties of helium might be connected with the statistics of the nuclei. An ideal Bose-Einstein gas was known to condense in momentum space rather than position space in such a way

that a finite fraction of the atoms are in the ground state at temperatures below some transition temperature.

Starting from the Bose-Einstein distribution law and conservation of the total number of particles, one replaces the discrete distribution by a continuous distribution with the ground state treated separately. It then turns out that the total number of particles are divided between the ground state and the excited states according to

$$N = (e^{\alpha} - 1)^{-1} + N(T/T_c)^{3/2} \left(F_{3/2}(\alpha)/F_{3/2}(0)\right) \qquad (20)$$

where the first term on the right represents the number of atoms in the ground state and the second is the number in the excited state. Here (α) is a parameter,

$$F_s(\alpha) = \frac{1}{\Gamma(s)} \int_0^{\infty} \frac{y^{s-1} dy}{\exp(y+\alpha)-1}$$

and $\Gamma(s)$ is the gamma function. (T_c) is the critical temperature

$$T_c = \frac{2\pi\hbar^2}{mk} \left(\frac{N}{2.612\ V}\right)^{2/3} \qquad (21)$$

For large (N) the character of the solutions to equation 20 changes sharply as one goes from $T > T_c$ to $T < T_c$. For $T < T_c$ there exists a solution for (α) of order (1/N). The number of atoms in the ground state becomes approximately

$$N_o \sim 1/\alpha \sim N(1-(T/T_c)^{3/2}) \qquad T < T_c$$

$$N_o \sim 0 \qquad T > T_c$$

Numerical evaluation of equation 21 for the critical temperature gives $T_c = 3.13^{\circ}K$, not too far from the observed transition temperature (lambda point) of $2.186^{\circ}K$ However, the number of atoms in the ground state is

experimentally observed to vary as $(T/T_c)^{5.6}$ rather than $(T/T_c)^{3/2}$ as predicted by equation 20. The specific heat variation and form of the lambda transition are also incorrectly predicted. Despite these difficulties the quantitative agreement of the transition temperature lead to the conviction that this mechanism was basically the one involved, and that deviations were probably due to small effects which could be included at a later time. The most important single prediction of this model was the failure of He^3 to become a superfluid. Inclusion of statistics must be an essential feature of any theory of helium.

b) Excitation spectrum

The most recent theories do include the statistics, either explicitly or implicitly. In order to fit the experimental data on specific heats and second sound velocity Landau (14) proposed that helium consists of a ground state of ideal fluid which flows frictionlessly and through which move excitations of two types. At low temperatures longitudinal phonons of energy $E = pc$, where (c) is the first sound velocity, are excited, leading to a Debye (T^3) contribution to the specific heat. At higher temperatures more complicated excitations called rotons are excited, which are separated by an energy gap, (Δ), from the phonons and which move with momentum (p) and effective mass (μ). Their spectrum is given in the neighborhood of the gap by

$$E(p) = \Delta + (p-p_o)^2/2\mu \qquad (22)$$

The specific heat and velocity of second sound can be calculated in terms of this energy spectrum. Values of the parameters chosen to obtain the best fit to the experimental data are (5):

$$\mu = 0.40\ m_{He}$$

$$p_o/\hbar = 2.03\ A^{-1}$$

$$\Delta/k = 9.6^{o}K$$

$$c = 240\ \text{meters/sec}$$

where (k) is Boltzmann's constant.

The energy spectrum has recently been measured using neutron diffraction techniques, and is found to yield a value $\Delta/k \sim 8.6^{o}$ K for the energy gap. The discrepancy may arise from treating the rotons as independent, and failing to include roton-roton interaction terms near the lambda point where the roton density is high.

The spectrum has also been computed from first principles by Feynman (8). He shows that rotons may be considered as made up of "smoke rings" consisting of a small number of atoms. The wave function for rotons is to first order of the form

$$\Psi = \sum e^{i\bar{K}\cdot\bar{R}}\ \varphi \qquad (23)$$

where (φ) is the ground state wave function for helium. Using a modification of this wave function which includes a backflow term Cohen (3) has obtained an energy gap $\Delta/k = 11.5 \pm 0.6^{o}K$, which is extremely close agreement for a variational calculation in such a complicated situation as exists in helium II.

For helium in macroscopic motion the wave function is modified and becomes

$$\Psi = e^{i\Sigma s(\bar{R}_i)}\ \varphi$$

where the flow velocity is given by the gradient of the phase

$$\bar{v} = \hbar/m\ \nabla s(\bar{R})$$

The flow described by this wave function is irrotational since the curl

of the velocity vanishes. However, for a multiply connected region the curl need not vanish. The only requirement is that the wave function be single valued. This requirement implies that for a path around some kind of hole the circulation may be quantized in units of (h/m) (8):

$$\oint \bar{v} \cdot d\bar{l} = 2\pi(\hbar/m)n = 2\pi(1.5 \times 10^{-4})n \quad cm^2/sec \qquad (24)$$

where (n) is an integer.

The fact that the product of a velocity times a distance is constant leads Feynman to suggest his correspondence principle that in any experiment involving superfluid flow the product of some characteristic length with some velocity will be invariant. This principle explains the lowest temperature results of Hollis-Hallett's oscillating disk experiments. It also leads to a predicted lift law in the present experiments.

c) Two fluid model

A phenomenological model for liquid helium II which contains features of the London model was proposed by Tisza (19). It is based upon a division of helium below the lambda point into two components, superfluid and normal fluid. The superfluid is identified with the ground state atoms of the London model while the normal fluid is identified with the atoms in excited states. The ground state helium is considered to possess no viscosity and to carry no entropy, so that all the observed viscosity and entropy effects are due to normal fluid alone.

This model is formalized by specifying a superfluid density (ρ_s) which moves with a velocity (v_s), and a normal fluid with density (ρ_n) moving with velocity (v_n). The sum of the separate densities

is the observed density of helium ($\rho_n + \rho_s = \rho$). The kinetic energy associated with the superfluid component is $\frac{1}{2}\rho_s v_s^2$ and with the normal component $\frac{1}{2}\rho_n v_n^2$.

The relative densities of superfluid and normal fluid vary with the temperature so that at the lambda point there exists only normal fluid and at absolute zero only superfluid. The entropy (s) is assumed to be carried entirely by the normal fluid and may be related to the value at the lambda point (s_λ) by $(s/s_\lambda) = (\rho_n/\rho)$.

Using this model Tisza predicted the existence of thermal waves, or second sound. Erroneous extrapolation of the above assumed variation of entropy with superfluid density to absolute zero led him to predict the vanishing of second sound velocity at absolute zero in contradiction to Landau's prediction (14) (later confirmed experimentally) that it should approach the limiting value $(c/3^{\frac{1}{2}})$ where (c) is the velocity of ordinary sound.

The two fluid model may be derived (6), (8) using the Bose-Einstein distribution. If there exist excitations in a moving fluid, the energy required for excitation formation may be found by considering moving and stationary coordinate systems. If the fluid velocity relative to the walls is $(\bar{v})$, the excitation energy (E) in the test system is given by (6)

$$E = E(\bar{p}) + \bar{p}\cdot\bar{v} \qquad (25)$$

where $E(\bar{p})$ is the energy measured by an observer in the moving system. If the excitations drift with momentum $(\bar{p})$, the average momentum carried by the excitations, $\langle\bar{p}\rangle$, may be found from the distribution function $n(E) = [\exp(E/kT)-1]^{-1}$ using the modified energy spectrum

(equation 25). Thus

$$\langle \bar{p} \rangle = \int \frac{\bar{p}}{\exp(1/kT)(E(\bar{p})-\bar{p}\cdot\bar{v})} \quad \frac{d^3\bar{p}}{(2\pi\hbar)^3} \tag{26}$$

Expanding to first order in (v) this may be written in the form $\langle \bar{p} \rangle = \rho_n v$, with (ρ_n) given by

$$\rho_n = (1/3kT) \int \frac{\exp(E(\bar{p})/kT)}{\left[\exp(E(\bar{p})/kT) - 1\right]^2} \quad \frac{p^2 d^3\bar{p}}{(2\pi\hbar)^3} \tag{27}$$

This value of (ρ_n) is in agreement with values determined from other considerations, and with experiments predicated upon the two fluid model. The superfluid density may then be defined by $\rho_s = \rho - \rho_n$.

By considering the motion of the excitations the complete two fluid model may be worked out in terms of first order expansions of the distribution functions. At high velocities second order terms would be expected to become important and the normal fluid density would then become a function of velocity. In practice the two fluid model deteriorates at velocities well below those predicted from this analysis.

The fundamental point is that the two fluid model does not possess any obvious physical interpretation. It is a useful tool derived from an approximation to the distribution function. Despite this it has proved extremely powerful for explaining the results of a large variety of experiments as well as for predicting the results of proposed experiments. It now forms such a basic part of the working theory of liquid helium that the usual procedure in explaining new effects is to attempt to add new terms to the two fluid equations of motion, rather than propose new models. It proves completely adequate for understanding the low velocity results of the present experiment.

APPENDIX II

KUTTA - JOUKOWSKI THEOREM

We assume the two dimensional complex potential function $w(z) = \varphi + i\psi$ to be given, where $z = x + iy$, (φ) is the potential function, and (ψ) is the stream function. The velocities in the (x) and (y) directions are given by $u = \frac{dx}{dt} = \frac{\partial \varphi}{\partial x}$ and $v = \frac{dy}{dt} = \frac{\partial \varphi}{\partial y}$ respectively. The Cauchy-Riemann equations

$$\frac{\partial \varphi}{\partial x} = \frac{\partial \psi}{\partial y} \qquad \text{and} \qquad \frac{\partial \varphi}{\partial y} = -\frac{\partial \psi}{\partial x}$$

are satisfied automatically and hence

$$\frac{dw}{dz} = \frac{\partial \varphi}{\partial x} + i\frac{\partial \psi}{\partial x} = \frac{\partial \psi}{\partial y} - i\frac{\partial \varphi}{\partial y} = u - iv$$

The pressure may be found at any point from Bernoulli's equation

$$p = H - \tfrac{1}{2}\rho(u^2 + v^2)$$

where (H) is a constant. The density will be taken to be constant.

The circulation about a wing is found by considering an arbitrary region surrounding it, and integrating:

$$\oint \frac{dw}{dz}\,dz = \int (u - iv)(dx + idy) = \int (udx + vdy) + i\int (udy - vdx) = C \quad (28)$$

where $\int (udx + vdy) = \oint \bar{v} \cdot d\bar{\ell} = C$, the circulation

and $\int (udy - vdx) = \int \bar{v} \cdot d\bar{A} = \Lambda = 0$, the volume outflow.

The volume outflow vanishes since there are no sources or sinks.

We expand $\frac{dw}{dz}$ as a power series about infinity

$$\frac{dw}{dz} = a + \frac{b}{z} + \frac{c}{z^2} + \cdots$$

where (-a) is the velocity vector at infinity

$$a = - v e^{-i\gamma}$$

if the flow approaches the wing at an angle (γ).

B is a pure imaginary number since by Cauchy's theorem and equation 28

$$\oint \frac{dw}{dz} dz = 2\pi i b = C$$

so

$$b = C/2\pi i$$

Writing an expression analogous to equation 28 for the momentum outflow we may equate the force transmitted across the boundary of the region to the rate of change of momentum in the region. Then

$$F_x - \int p dy - \int \rho u(udy - vdx) = 0$$

and

$$F_y - \int p dx - \int \rho v(udy - vdx) = 0$$

so

$$\begin{aligned} F_x - iF_y &= - \int p(dy - idx) - \int \rho(u - iv)(udy - vdx) \\ &= \tfrac{1}{2} \rho \int (u^2 - v^2 - 2iuv)(idx - dy) \end{aligned}$$

However

$$\frac{dw}{dz} = u - iv$$

so

$$F_x - iF_y = \tfrac{1}{2}\rho i \oint (\frac{dw}{dz})^2 dz$$

Now expand $(\frac{dw}{dz})^2$ and use Cauchy's theorem

$$(\frac{dw}{dz})^2 = a^2 + \frac{2ab}{z} + \frac{b^2 - 2ac}{z^2} + \cdots$$

$$F_x - iF_y = \tfrac{1}{2}\rho i \oint (\frac{dw}{dz})^2 dz = \tfrac{1}{2}\rho i (2ab)(2\pi i) = - \rho C v i e^{i\gamma}$$

The magnitude of the lift force is

$$L = \rho v C$$

and the direction is normal to the velocity at infinity. The drag force therefore vanishes.

APPENDIX III

FLOW ABOUT AN ELLIPTIC CYLINDER WITH ARBITRARY CIRCULATION

Consider an ellipse of major axis (w) and minor axis (n), making an angle of attack (γ) with a fluid flowing uniformly with velocity (v) at infinity. We use the elliptic cylindrical coordinates

$$x = \tfrac{1}{2}a \cosh\mu \cos\theta$$

$$y = \tfrac{1}{2}a \sinh\mu \sin\theta$$

The loci μ = constant are ellipses of major axis ($a \cosh\mu$) and minor axis ($a \sinh\mu$).

Let $w = \mu + i\theta = \cosh^{-1}(2z/a)$ and define the complex potential (ψ). The velocity may be found at any point:

$$v = \nabla\psi = \left|\frac{dw}{dz}\right|\left(\bar{e}_\mu \frac{\partial\psi}{\partial\mu} + \bar{e}_\theta \frac{\partial\psi}{\partial\theta}\right)$$

$$= \frac{2/a}{(\sinh^2\mu + \sin^2\theta)^{\frac{1}{2}}}\left(\bar{e}_\mu \frac{\partial\psi}{\partial\mu} + \bar{e}_\theta \frac{\partial\psi}{\partial\theta}\right)$$

where ($\bar{e}_\mu$) and ($\bar{e}_\theta$) are unit vectors in the (μ) and (θ) directions. The uniform flow approaching the ellipse at angle (γ) is given by

$$\psi = v(x\cos\gamma + y\sin\gamma) = \frac{av}{2}(\cosh\mu\cos\theta\cos\gamma + \sinh\mu\sin\theta\sin\gamma)$$

To this can be added any solutions which vanish at infinity, such as $e^{-\mu}\cos\theta$ and $e^{-\mu}\sin\theta$, so that

$$\psi = \frac{av}{2}(\cosh\mu\cos\theta\cos\gamma + \sinh\mu\sin\theta\sin\gamma + Ae^{-\mu}\cos\theta + Be^{-\mu}\sin\theta)$$

The boundary condition to be applied is the vanishing of the normal gradient of (ψ) at $\mu = \mu_0$.

Then

$$\left|\frac{dw}{dz}\right|\left(\frac{\partial\psi}{\partial\mu}\right)_{\mu=\mu_0} = 0$$

and

$$0 = \cos\theta(\sinh\mu_o \cos\gamma - Ae^{-\mu_o}) + \sin\theta(\cosh\mu_o \sin\gamma - Be^{-\mu_o})$$

Equate terms separately to zero to find (A) and (B).

$$A = e^{\mu_o} \sinh\mu_o \cos\gamma$$

$$B = e^{\mu_o} \cosh\mu_o \sin\gamma$$

Now add a circulation term $(C/2\pi)\theta$ so $\psi = \psi_o + (C/2\pi)\theta$. The tangential velocity (v_T) at the surface of the ellipse ($\mu = \mu_o$) is

$$v_T = v(\sinh^2\mu_o + \sin^2\theta)^{-\frac{1}{2}} \left[(2/av)(C/2\pi)\right. \qquad (29)$$
$$\left. - \cos\gamma \sin\theta(\cosh\mu_o + \sinh\mu_o) + \sin\gamma\cos\theta(\sinh\mu_o + \cosh\mu_o)\right]$$

Substitution for the major axis $w = a\cosh\mu_o$ and for the minor axis $n = a\sinh\mu_o$ allows this to be written

$$v_T = (n^2 + (w^2-n^2)\sin^2\theta)^{-\frac{1}{2}} (C/\pi + v(w+n)\sin(\gamma - \theta))$$

which may be evaluated at $\theta = 0, \pi, \pi/2$, and $3\pi/2$ (front, rear, top, and bottom respectively) to yield equations 9a-9d.

To show that this circulation is the same as that used in equation 7 ($C = \oint \bar{v}\cdot d\bar{l}$) we evaluate $\int v_T dl$. Let $\mu \to \infty$. Then the elliptical coordinates approach polar coordinates.

$$r = (x^2 + y^2)^{\frac{1}{2}} \longrightarrow (a/2)(e^{\mu}/2)$$

$$\tan\varphi = y/x \longrightarrow \tan\theta$$

Equation 29 becomes (dropping the subscript on (μ_o))

$$v_T = (4/a)e^{-\mu}\left[(C/2\pi) + (av/4)\, e^{\mu} \sin(\gamma - \theta)\right]$$
$$= (C/2\pi r) - v\sin(\gamma - \theta)$$

Then

$$\oint v_T\, dl = \int_o^{2\pi} v_T\, r\, d\varphi$$

The second term vanishes upon integration. The term involving (C) becomes

$$\int (C/2\pi r)\, r d\varphi = C$$

APPENDIX IV

APPLICATION OF CORRESPONDENCE PRINCIPLES TO WINGS

Consider the vicinity of the trailing edge of a two dimensional wing of arbitrary cross section. We define the quantities:

- a stagnation point with no circulation
- b stagnation point with the Kutta condition satisfied
- y a coordinate which moves from (b) to (a)
- y_a maximum value of (y). $y=y_a$ at position (a)
- v free stream velocity at infinity
- v' local velocity at (y) corresponding to (v) (with no circulation)
- w' local velocity at (y) corresponding to (a) circulation (C') about the wing and v = 0
- v_c' maximum local velocity when superfluid flow breaks down (this occurs at position b)
- v_c free stream velocity corresponding to (v_c')
- C classical circulation with Kutta condition satisfied
- $L_{classical} = \rho v C$

As the circulation velocity (w') varies from zero to (v') the stagnation point moves linearly along the surface from (a) to (b) (fig. 14). Then

$$y/y_a = 1 - w'/v' \tag{30}$$

The local velocity at (y) is (v' - w')

The correspondence principles require that the product of a characteristic velocity times a distance raised to some power be constant (equation 17). We choose as a velocity the local velocity (v_t') at point (b) and as a distance the distance (y) between (b), the stagnation point with the Kutta condition satisfied, and (y), the stagnation point with circulation (C') present (fig. 14). The correspondence principle then becomes

$$v_a\, y^{1/s} = (v' - w')\, y^{1/s} = \text{constant}$$

The constant may be evaluated from the conditions when superfluid flow

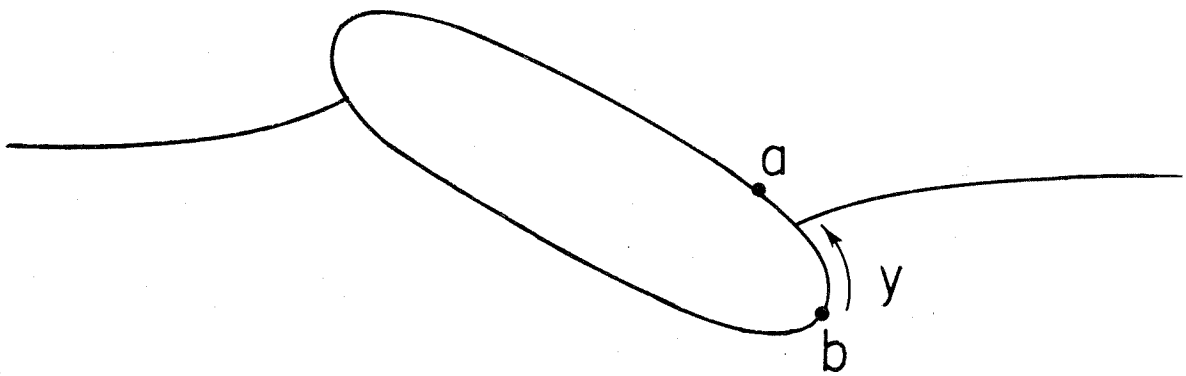

FIGURE FOR THE APPLICATION OF THE CORRESPONDENCE PRINCIPLE $Vy^{1/s} = \text{CONSTANT}$ TO THE LIFT ON AN AIRFOIL

FIGURE 14

first breaks down

$$v_c' \, y_a^{1/s} = \text{constant}$$

so

$$(v' - w') = v_c' \, (y_a/y)^{1/s}$$

Using equation 30 we find

$$(v' - w') = v_c' \, (1 - w'/v')^{-1/s}$$

from which

$$w' = v' \left[1 - (v_c'/v')^{s/(s+1)} \right]$$

Since the classical circulation is proportional to (v'), $C = \text{const}\ (v')$. The new circulation is proportional to (w') with the same constant: $C' = \text{const}\ (w')$.

Also $(v_c'/v') = (v_c/v)$. Therefore the expected lift becomes

$$L = \rho v C' = \rho v C(w'/v') = \rho v C \left[1 - (v_c/v)^{s/(s+1)} \right]$$

or

$$L = L_{\text{classical}} \left[1 - (v_c/v)^{s/(s+1)} \right] \qquad (31)$$

If we now define $g = v/v_c$ and $P = L/L_{\text{classical}}$, we may write equation 31 in dimensionless form

$$P_s = g^2 \left[1 - (1/g)^{s/(s+1)} \right] \qquad g \geq 1$$

As $s \to \infty$, $P_s \to g^2(1 - 1/g)$ which is the simple modification of the Kutta condition proposed in Part VI. The form of the law for $s = 1$ and $s = 2$ does not differ appreciably from this. (Fig. 15) shows (P_s/P_∞) for $s = 1$ and $s = 2$. For $1.5 < g < 3$, $P_1/P_\infty = .59$ to within 6% while $P_2/P_\infty = .74$ to within 5.5%.

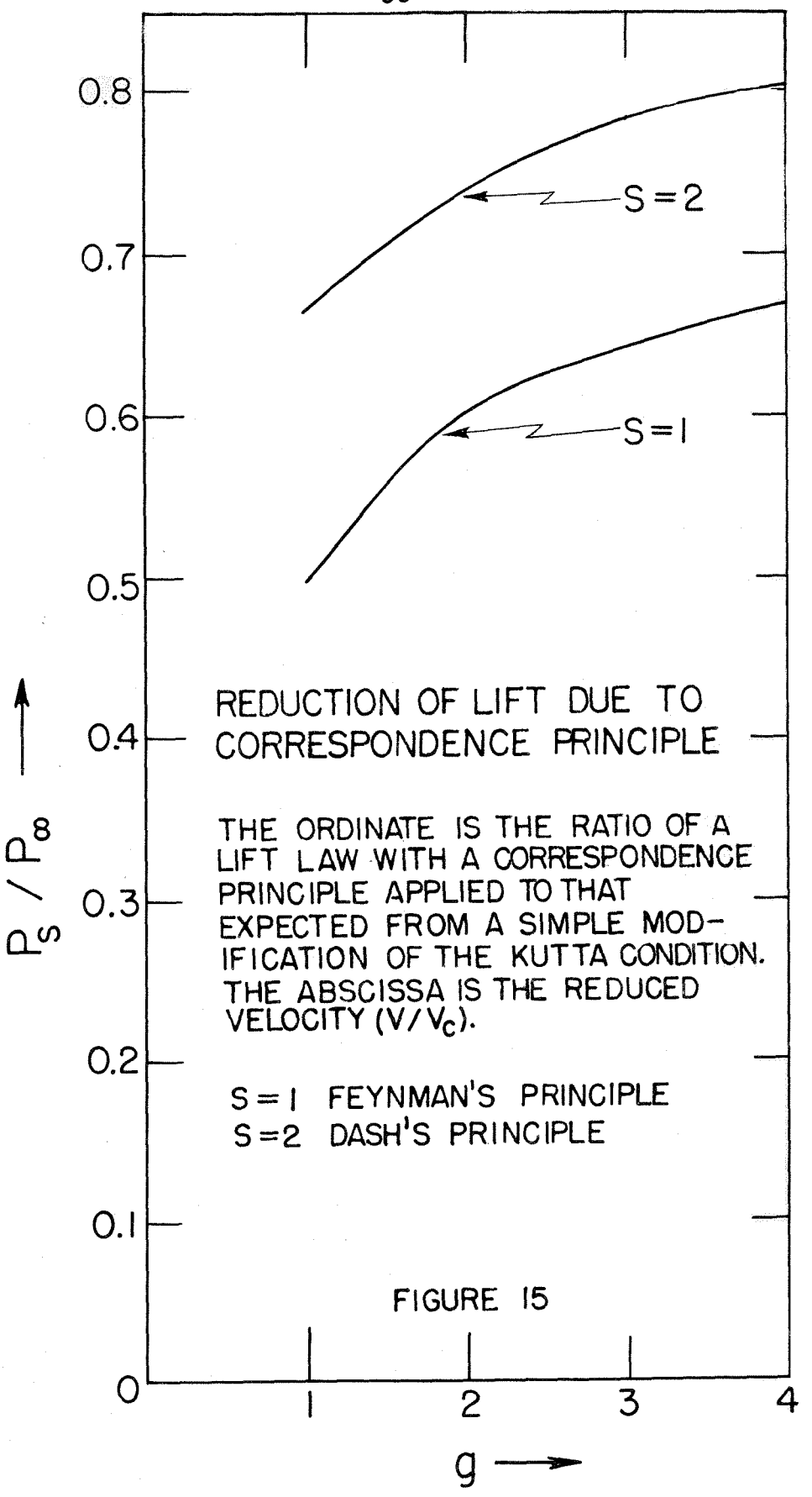
0.8
0.7
0.6
0.5
0.4
0.3
0.2
0.1
0
1
2
3
4
g
P_S / P^8
S = 2
S = 1
REDUCTION OF LIFT DUE TO CORRESPONDENCE PRINCIPLE
THE ORDINATE IS THE RATIO OF A LIFT LAW WITH A CORRESPONDENCE PRINCIPLE APPLIED TO THAT EXPECTED FROM A SIMPLE MODIFICATION OF THE KUTTA CONDITION. THE ABSCISSA IS THE REDUCED VELOCITY (V/V_c).
S = 1 FEYNMAN'S PRINCIPLE
S = 2 DASH'S PRINCIPLE

FIGURE 15

APPENDIX V

EFFECT OF LEAKAGE

We show how leakage through the carborundum barrier of the superfluid wind tunnel creates a counterflow of normal fluid and an increase of superfluid flow. These contributions modify the lift equations for an airfoil.

a) Effect of leakage on tunnel

Let the total heat input be $(\dot{H})$ and the tunnel area one square centimeter. A certain amount $\dot{H}_c$ (T) of heat is lost through evaporation, etc. This has been experimentally observed to correspond to a fixed superfluid flow velocity (v_1) (v_1 = .23 cm/sec in the tunnel used) (fig. 4). Then H_c (T) = $v_c/(\rho_s sT)$ where v_c does not depend on temperature. The remaining heat input $H_1 = H - H_c$ (T) is divided between a fraction (γ_o) used in the normal wind tunnel manner and a fraction $(1 - \gamma_o)$ lost by reverse leakage through the carborundum.

This fraction appears as an extra heat source in the tunnel. Should the tunnel entrance (S', fig. 1) be thermally blocked the temperature in the test section must rise. We assume (S') not to form a thermal barrier.

The tunnel velocity calculated from the pitot tube level difference (v_{sp}) will be based only on the heat $(\gamma_o \dot{H}_1)$:

$$v_{sp} = \gamma_o \dot{H}_1 / \rho_s sT \qquad (32)$$

The leakage heat $(1 - \gamma_o)\dot{H}_1$ creates a counterflow of normal fluid (v_n) in the tunnel

$$v_n = (1 - \gamma_o)\dot{H}_1/\rho sT = ((1 - \gamma_o)/\gamma_o)(\rho_s/\rho)v_{sp} \qquad (33)$$

and an attendant excess flow of superfluid (v_{s1}) found by momentum conservation

$$\rho_s v_{s1} = \rho_n v_n$$

so

$$v_{s1} = (\rho_n/\rho_s)v_n = (\rho_n/\rho)((1 - \gamma_o)/\gamma_o) v_{sp} \qquad (34)$$

The total superfluid velocity in the tunnel is

$$v_s = v_{sp} + v_{s1} = \left[1 + (\rho_n/\rho)((1 - \gamma_o)/\gamma_o)\right] v_{sp} \qquad (35)$$

replacing (ρ_n/ρ) by (x) and (ρ_s/ρ) by (1-x) in equations 33 and 35 yields equations 4 and 5 of the text.

The value of (γ_o) may be found from curves similar to (fig. 4). The tunnel velocity of superfluid based on power input alone (v_H)

$$v_H = \dot{H}/\rho_s sT$$

must be modified by subtraction of the heat lost by evaporation, etc., H_c (T). The corrected tunnel velocity (v_{Hc}) then becomes

$$v_{Hc} = \dot{H}/\rho_s sT - v_1 = \dot{H}/\rho_s sT - H_c(T)/\rho_s sT = \dot{H}_1/\rho_s sT$$

The slope of (fig. 4) would then be

$$v_{Hc}/v_{sp} = 1/\gamma_o \qquad (36)$$

b) Effect of leakage on the lift laws.

We use the notation of Parts IV and VI. The normal fluid counterflow will give a contribution (Ln) to the lift, but in a direction opposite to that of the superfluid

$$L_n = A' \rho_n v_n$$

The superfluid gives a contribution (Ls)

$$L_s = m\rho_s v_s(v_s - v_c) \qquad (37)$$

The final lift is

$$L = L_s - L_n = m\rho_s v_s^2 - m\rho_s v_s v_c - A'\rho_n v_n^2$$

Using equations 33 and 35 to express (v_s) and (v_n) in terms of the superfluid velocity measured at the pitot tubes (v_{sp}), we find

$$L = \rho v_{sp}\left\{\left[m(1-x)(1+x\gamma)^2 - A'\gamma^2 x(1-x)^2\right] v_{sp} - m(1-x)(1+x\gamma)v_c\right\} \quad (38)$$

which is still of the form of equation 37 but with new parameters. Here we use the abbreviation $\gamma = (1 - \gamma_o)/\gamma_o$. For low velocities a parabolic negative lift would be expected from the normal fluid leakage. The effective critical velocity (v_{ce}) (value of v_{sp} at axis crossing) must be computed at each temperature. Any expected temperature variation of (m) or (v_c) may be included. However, even assuming (m) and (v_c) constant the temperature variation of equation 38 is complicated. In the limit as $x \to o(\rho_s/\rho \to 1)$ the leakage contribution vanishes and

$$L \to m\rho_s v_{sp}(v_{sp} - v_c)$$

$$v_{ce} \to v_c$$

In the limit as $x \to 1(\rho_s/\rho \to 0)$, (assuming $\gamma << 1$)

$$L \to m\rho_s(1+\gamma)^2 v_{sp}\left(v_{sp} - \frac{v_c}{1+\gamma}\right) = (m\rho_s/\gamma_o^2)v_{sp}(v_{sp} - \gamma_o v_c)$$

$$v_{ce} \to v_c/(1+\gamma) = \gamma_o v_c$$

For (γ) of the order of one tenth the influence of leakage could not be detected with the available experimental accuracy.

References

1. Alembert, Essai d'une Nouvelle Theorie de la Resistance des Fluides, Paris, (1752)

2. Allen, J. F. and Misener, A. D., Proc. Royal Soc. London, A 172, 467, (1939)

3. Cohen, M., Thesis, California Institute of Technology, (1956)

4. Dash, G., Phys. Rev., 94, 825 and 1091, (1954)

5. de Klerk, D. Hudson, R. P., and Pellam, J. R., Phys. Rev., 93, 28, (1954)

6. Dingle, R. B., Advances in Physics, 1, 112, (1952)

7. Durand, W. F., Aerodynamic Theory, Vol. II.

8. Feynman, R. P., in Progress in Low Temperature Physics, C. F. Gorter, Editor, North-Holland Publishing Company, Amsterdam, (1955)

9. Hall, H. E., Phil. Trans. Royal Soc., 250, 359, (1957)

10. Hollis-Hallett, A. C., Proc. Phys. Soc. London, A 63, 1367, (1950)
Proc. Royal Soc. A 210, 404, (1952)

11. Kapitza, P. L., J. Phys. USSR, 4, 181, (1941)
5, 59, (1941)

12. Koehler, T., Private Communication

13. Lamb, H., Hydrodynamics, Dover, New York, (1945)

14. Landau, L., J. Phys. USSR, 5, 71, (1941)

15. Onsager, Nuov. Cim., 6, Supp. 2, 249, (1949)

16. Pellam, J. R., in Progress in Low Temperature Physics, C. J. Gorter, Editor, North-Holland Publishing Company, Amsterdam, (1955)

17. Simon, F., Nature, 133, 529, (1934)

18. Strong, J., Procedures in Experimental Physics, Prentice Hall, New York, (1938)

19. Tisza, C. R., Phys. Rev., 72, 838, (1947)

20. Wick, B., Study of the Subsonic Forces and Moments on an Inclined Plate of Infinite Span, NACA Technical Note 3221, Washington, (1954)

21. Winkel, P., Delsing, A. M. G., and Poll, J. D., Commun. Kammerlingh Onnes Lab., Leiden No 299b, Physica 21, 331, (1955)